Multi-scale characterization of industrial infrastructure vulnerability to multiple hazards in their territories

Journal of Safety Science and Resilience 6 (2025) 297–315

Contents lists available at ScienceDirect

Journal of Safety Science and Resilience

journal homepage: www.keaipublishing.com/en/journals/journal-of-safety-science-and-resilience/

Multi-scale characterization of industrial infrastructure vulnerability to multiple hazards in their territories

David Javier Castro Rodriguez *, Antonello A. Barresi, Micaela Demichela

Department of Applied Science and Technology, Politecnico di Torino, Torino, 10129, Italy

ARTICLE INFO

Keywords:
Multi-hazard
Major hazard industries
NaTech
Resilience
Territorial vulnerability

ABSTRACT

Directive 2022/2557 from the European Commission aims to enhance the resilience of critical entities in Europe by integrating with existing European legislation, but it lacks explicit guidance on addressing vulnerabilities. Specifically, major hazard industries (MHIs) are critical infrastructures that face unique risks arising from the interactions of natural and technological hazards (NaTech events); nevertheless, existing policies frequently overlook the potential vulnerabilities of process plants to these complex phenomena. The goal of this research was to systematically characterize the vulnerability of industrial critical infrastructures (ICIs) to various hazards in their territories. A multi-scale procedure was implemented in the Italian context as a case study, where spatial analyses were developed using open data. Starting from the Italian national inventory, the MHIs were clustered in industrial macro-sectors and represented nationally by regions, relating their distribution to meteorological or geophysical data of interest. At the regional scale, the MHIs of the Piedmont Region were represented as punctual elements, associating the population within potential damage zones by province. At the municipal scale, a previously validated multi-hazard tool for vulnerability assessment was then tailored to a reduced scale for specific applications in an industrial context. This adaptation, which considers the two-way interaction between an energetic critical infrastructure and various hazards in its surroundings, delivers a spatial vulnerability profile that may complement the probabilistic analysis of industrial incidental scenarios. In summary, this framework may raise the stakeholders awareness at various levels and with different interests within the industrial accident control decision-making chain, from operators to competent authorities.

1. Introduction

The European Commission has released Directive (EU) 2022/2557[1] to strengthen the resilience of critical entities, establishing that Member States must identify entities that provide essential services that might be disrupted by a disaster, evaluate the risks associated with the infrastructure, and make national strategies by January 2026. Based on these risk evaluations, critical entities should adopt relevant organizational and technological steps, including steps to mitigate vulnerabilities, to guarantee their resilience. However, the directive does not include any explicit instructions or methodology on how vulnerabilities should be handled.

Moreover, the (EU) 2022/2557 directive points out in Article 5 that when Member States conduct risk assessments, they must proceed in compliance with the requirements of the applicable sector-specific European Union legislation, specifically mentioning 2012/18/EU[2] Directive (Seveso III), and it is explicitly stated that all relevant natural and man-made hazards that could lead to an accident should be taken into consideration. However, when considering the potential impact of natural hazards, the 2012/18/EU Directive is limited to mentioning earthquakes and floods, while no reference to other factors is explicit.

The diverse legal, geographical, and cultural circumstances among the European Member States significantly impact the effectiveness of implementing the Seveso III Directive into national policies [1]. For example, in France and Italy, which together host around 20 % of Seveso establishments in Europe [2], the criteria for land use planning (LUP) are applied based on potential damage zones, which consider the external elements that could be impacted in the case of technological events [3]. This approach leads operators to consider the environment

* Corresponding author.
E-mail address: david.castro@polito.it (D.J. Castro Rodriguez).

[1] Directive 2022/2557 of the European Parliament and of the Council on the resilience of critical entities and repealing Council Directive 2008/114/EC.

[2] Directive 2012/18/EU on the control of major-accident hazards involving dangerous substances, amending and subsequently repealing Council Directive 96/82/EC.

https://doi.org/10.1016/j.jnlssr.2024.11.004
Received 25 September 2024; Received in revised form 12 November 2024; Accepted 12 November 2024
Available online 14 February 2025

Abbreviations

FID	specific Field IDentifier
GIS	Geographical Information Systems
ICIs	Industrial Critical Infrastructures
LUP	Land Use Planning
MHIs	Major Hazards Industries
NaTech	Technological scenarios involving the release of hazardous materials caused by a natural hazard
SETSs	Socio-Ecological and Technological Systems.

primarily as a potential receptor of impacts rather than as a potential source of disruptions [4]. Consequently, the reverse direction, where industrial plants can be seen as potential targets of the interaction of concomitant hazards inherent to their surrounding territories, is repeatedly overlooked under the 2012/18/EU Directive [5].

The necessity for states to document and provide managers with information on the frequency of combined natural and technological events impacting their regions has been emphasized for decades [6]. Additionally, new and legacy industries, coupled with climate change, present unique risks to communities living near the industry, increasing their vulnerability [7]. However, the interplay between technological scenarios and natural hazards that could also emerge at the plant location is not well addressed from a regulatory point of view in Europe [4]. Consequently, these complex interactions derived in multi-hazard scenarios are often underestimated by operators during the identification of risk inventories [8]. Additionally, it is acknowledged that some European Member States have limited the response to the catastrophic impact of natural disasters to some sectorial programs issued by different authorities with different methodologies [9,10]. Therefore, decision-makers assess major hazards separately, using information generated from diverse methodologies applied at heterogenous scales.

Hence, the vulnerabilities of essential industrial assets to the multiple hazards that exist in their territories are often not well assessed, triggering the following research question: “Can the implementation of spatially advanced methods improve the vulnerability characterization of industrial critical infrastructures (ICIs) with respect to various hazards inherent to their territories”? To address this issue, a location-based procedure was designed to systematically characterize the ICIs vulnerability to hazards in their territories. This analysis examines different perspectives on the relationship between industrial characteristics and relevant hazards, utilizing both real and simulated scenarios across different scales within the Italian setting.

2. Theoretical foundations

2.1. Key concepts to approach the interplay between ICIs within a multi-hazard framework

It is essential to have a more comprehensive understanding of how the interplay between ICIs and multiple hazards in their territories can lead to critical outcomes. To handle the complexity of these socio-ecological and technological systems (SETSs), it is crucial to introduce the concept of multi-hazard, which means “(1) the selection of multiple major hazards that the country faces, and (2) the specific contexts where hazardous events may occur simultaneously, cascadingly or cumulatively over time, and taking into account the potential interrelated effects” [11].

According to the previous concept, the focus is centered on a peculiar type of multi-hazard, also known as NaTech, where technological accidents involving the release of hazardous materials are caused by natural hazards [12]. The interrelationship between the elements within the NaTech concept, such as “natural hazards”, “hazardous materials”, and “technological hazards”, can be expanded, combining the terminology for disaster risk reduction and process safety [11–13]. In a wider sense, we may deal with a loss of containment of biological, chemical, radiological, or nuclear agents originating in industrial assets from failures in technological conditions or infrastructure, triggered by a single natural process or phenomenon, or a chain of them. The technological scenarios generated by NaTech events have disastrous consequences. They can result in death, injury, illness, or other health impacts, as well as property damage, loss of livelihoods and services, social and economic disruption, or environmental damage. Remarkably, there exists a condition determined by inherent characteristics contextualized to the territory of concern that defines susceptibility to the impacts of hazards.

Given the previously addressed complexity of NaTech events, holistic approaches that integrate advanced methods alongside an interdisciplinary perspective at different scales are crucial for addressing challenges and mainstreaming opportunities in the fields of process safety, sustainability, and disaster prevention. Within this context, resilience emerges as a central topic in the debate on hazards affecting SETSs [14].

Resilience is the result of several processes occurring at different scales, both within and between circumstances of inherent vulnerability. These processes involve factors such as biophysical and socioeconomic features, infrastructure, land use, built environment, as well as external climatic and disaster threats [15].

Several authors have proposed that resilience principles are closely linked to the adoption of a holistic safety perspective for complex systems [16–20]. However, this approach is a broadly employed concept with different definitions and views depending on the field and context of interest [21,22].

For instance, resilience could be considered as a holistic way of thinking, as a performance, or as a system capability [14]. Similarly, the resilience evaluation process has two main categories: qualitative and quantitative. The qualitative category has two subcategories: conceptual frameworks for best practices and semiquantitative indices for expert assessments of various qualitative aspects. On the other hand, there are also two subcategories of quantitative methodologies: general resilience approaches that evaluate resilience across applications and structural-based modeling approaches that model domain-specific resilience components [21].

Due to the varied connections between resilience concepts and practical methods, this research will examine how resilience is addressed in the context of ICIs and the transposed Seveso legal framework for European Member States. This analysis will help clarify how the term resilience will be approached in this study.

First, in the field of process industry, even if resilience has been conceptualized as the next level of process safety and risk management method evolution [23], it is recognized that the advancement of resilience-based approaches has been limited, mainly due to a lack of clarity of the conceptual links between resilience principles and practical procedures [24]. In particular, the concept of resilience engineering has been actively developed since 2004 and has been successfully applied to accident investigations and risk assurance in several industrial domains [25]. This perspective enables proactive identification of potential emergent scenarios caused by interdependent components and mutual interactions and enables adaptation to the repercussions that result from increasingly sophisticated technology and complex organizations [26]. For example, engineering resilience-based strategies provide probabilistic predictions to learn from past experiences, which are useful to increase awareness and preparedness for facing vulnerable situations or elements.

Second, the emerging idea of territorial resilience is introduced as a concept capable of supporting the decision-making process, together with the necessary tools for identifying multiple vulnerabilities and guiding the transformation of SETSs [14]. The flexibility of territorial resilience connects many fields, disciplines, sectors, and stakeholders, providing a valuable concept for addressing complex problem-solving

phenomena and offering interventions [14,27]. In this approach, advanced mathematical and statistical methods, combined with place-based techniques that utilize Geographical Information Systems (GIS), are recommended. These tools can identify vulnerabilities as a first step, support decision-making processes, and ultimately guide the long-term transformation of SETSs while addressing their inherent complexity.

Third, another perspective of resilience is used in critical infrastructure systems where resilience analysis is divided into three phases that are based on the disruption profile approach [23,28]. It implies actions or impacts before, during, or after a disturbance. For better understanding, Fig. 1 illustrates the resilience approach by showcasing key concepts based on system functionality performance and the disruption profile. This classification provides a clear framework for analyzing resilience, aligning both the traditional pillars of resilience engineering and the territorial resilience approach.

Fig. 1(a) illustrates three marked phases, the first one, the awareness phase, involves promptly identifying vulnerabilities within the system to prevent potential disruptions. Vulnerability in the context of multi-hazards is generally conceptualized as a function of exposure, sensitivity, and adaptive capacity [15]. This concept refers to the condition that is determined by physical, socio-economic, and environmental contexts and processes that increase the system element predisposition (susceptibility) to be damaged punctually by hazardous events or continuous pressures over time [30].

After a significant event disrupts the normal system functionality, resilience is the intrinsic quality characteristic that allows the system to withstand functionality degradation and return to its pre-disruption performance level, while the disruptive performance of the system can be broken down into two phases: mitigation and recovery. First, the mitigation phase relies on accurately understanding the vulnerable conditions identified during the awareness phase and then taking appropriate action to absorb the impact of disruptive events. In the process industry, this involves strategies to enhance robustness, such as implementing inherently safer designs [31,32] and strengthening safety barrier responses [33–35], to mitigate disruptive impacts, resulting in less intervention during emergency responses of SETSs [36]. Subsequently, the recovery phase is conceived to take actions or efforts required to return to a new normal state by reducing response time and hence strongly reducing the likelihood of severe consequences (rehabilitation or restoration strategies).

Finally, the new normal state can vary across a spectrum of potential outcomes depending on the level of resilience attained during the disruption. Fig. 1(b) shows the state of the system after disruptions (better, similar, or worse performance compared to before the disruption). Additionally, the system may completely lose its functionality in the absence of resilience.

Throughout the building resilience process, the development and integration of policies for climate change adaptation, land use regulation, and disaster risk management can jointly impact the outcomes of vulnerability [15]. In this context, identifying vulnerabilities is often seen as the counterpart of building resilience [14], or at least a common stage of diverse frameworks to strengthen resilience [15]. Therefore, understanding vulnerability is considered the cornerstone for enhancing resilience by focusing on managing susceptibility during the normal performance of the system.

2.2. The concept of vulnerability within the control of major-accident hazards

According to the last public report on the implementation and efficient functioning of the Seveso III Directive, 11,776 establishments were registered in the different European Member States, with proportions of 43 % and 57 % for upper-tier establishments (UTE) and lower-tier establishments (LTE), respectively [2]. Since Italy ranked third among the Member States with a higher number of establishments, it was selected as a representative case study, owning slightly above 8 % of the European total, with 471 LTE and 507 UTE [37].

Italy fully transposed the requirements of the 2012/18/EU Directive with the Legislative Decree n.105 of June 26, 2015.[3] This decree follows the same structure, technical requirements, guidelines, and rules as the current implementation of the Seveso III Directive [38]. It makes some useful and necessary changes to make it work with Italian law and the government system. For example, supplementary technical annexes were introduced to complement European regulations with national guidelines. These include: i) directives for implementing the safety management system to prevent major accidents; ii) criteria, data, and information for creating and assessing the safety report; iii) standards for identifying facilities where a domino effect could occur, and for recognizing areas with a high concentration of facilities; iv) identification of modifications in facilities, storage units, processes, or the nature, physical form, or quantities of hazardous substances; and v) regulations governing personnel consultation regarding internal emergency plans (PEI) and external emergency plans (PEE), among others.

As introduced above, increasing vulnerability awareness represents a cornerstone for building resilience in complex systems. Specifically, the concept of vulnerability within Legislative Decree 105/15 is predominantly linked to the processes regulated by the Directive of the Minister for Civil Protection and Sea Policies of December 7, 2022,[4] regarding formulation, information, and external emergency plan testing (Art. 21) as well as land use and urban planning tools (Art. 22) specifically regulated under the Ministerial Decree of 09/05/2001[5] (LUP tool). However, one perspective is overlooked: the potential impacts of natural hazards linked to territorial characteristics on vulnerable industrial assets are not addressed in the LUP tool. These hazards are only briefly mentioned in the Ministerial Directive of 07/12/2022, which explicitly acknowledges that the external emergency guidelines are inadequate for managing NaTech events.

In Italy, the management of natural hazards is addressed through sector-specific plans for major natural risks. These plans are integrated into city plans and municipal emergency plans, which are prepared by municipalities responsible for direct land use management. Then, decision-makers are involved not only with assessing individual hazards that threaten exposed areas or elements, but also with evaluating the interactions of these factors in the absence of methodologies for systemic analysis [10,13]. Regarding the multi-risk available methods in urban areas, they focus on risk mitigation without considering interactions with technological risks [13]. In addition, previous researchers have underscored that those methods used at large or medium scales might be too general to work at a plant scale [39,40].

3. Methodological framework to characterize NaTech vulnerability between ICIs and their multi-hazard territorial contexts

To address the shortcomings discussed previously, the bidirectional

[3] Legislative Decree No. 105 of June 26, 2015, "Implementation of Directive 2012/18/EU on the control of major-accident hazards involving dangerous substances." Italian Official Gazette General Series No. 161 14/07/2015-Suppl. Ordinary No. 38.

[4] Directive of the Minister for Civil Protection and Sea Policies of December 7, 2022 - Part 1-"Guidelines for the preparation of the external emergency plan," Part 2-"Guidelines for information to the population," and Part 3-"Guidelines for the testing of external emergency plans"- pursuant to Article 21, Paragraph 7 of Legislative Decree No. 105 of June 26, 2015, "Implementation of Directive 2012/18/EU on the control of major-accident hazards involving dangerous substances." Italian Official Gazette No. 31, February 7, 2023.

[5] Ministry of Public Works Decree of May 9, 2001 "Minimum safety requirements in urban and territorial planning for areas affected by establishments at risk of major accidents." Italian Official Gazette No. 138 16/06/-Ordinary Supplement No. 151.

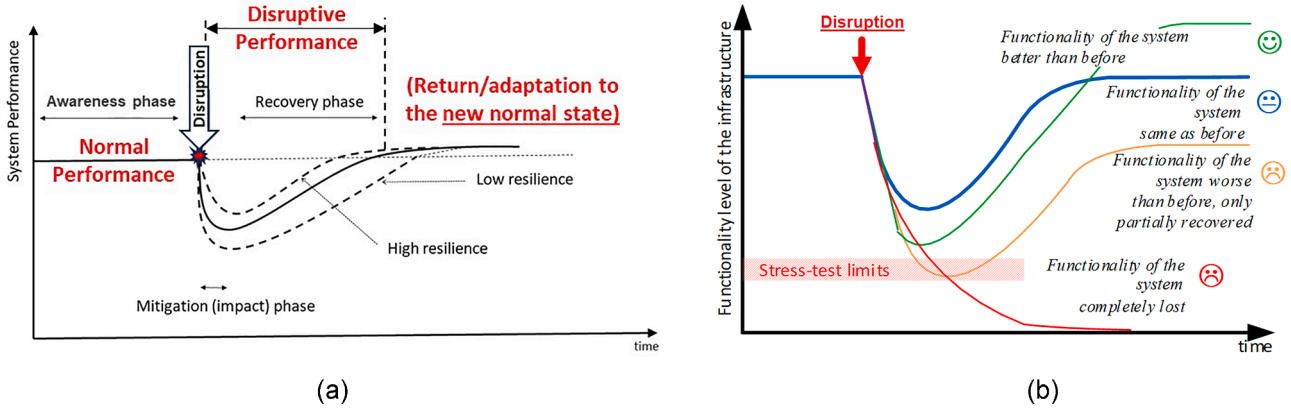

Fig. 1. Resilience concept representation based on the system performance. (a) System performance in three-phases based on the disruption profile. (b) Possible scenarios of system functionalities exposed to a disruptive event. Source: modified from [29].

relationship between ICIs and their multi-hazard territorial context was conceptualized focusing on the occurrence of NaTech events. Fig. 2 relates all these complex phenomena in a framework defined as the function-location approach.

The function-location approach conceptualizes the occurrence of NaTech events as the potential result of the intersection between the vulnerabilities belonging to the technological attributes of ICIs, and the territorial vulnerability to multiple natural factors in their surroundings. The functional and location factors are further subdivided as described below.

The left side in Fig. 2 corresponds with the technological vulnerabilities characterized by the functional attributes subdivided into "industrial infrastructure" and "dangerous substances." Modeling of technological vulnerabilities has been detailed in previous works [41, 42]. However, since disaster intensity, frequency, and impact extension are rarely recorded in industrial databases [8,43], their influence on potential NaTech consequences is difficult to quantify.

Therefore, the location factors on the right side of Fig. 2 refer to the geophysical, socio-economic, and environmental factors that increase the susceptibility of a territory to the impacts of natural hazards. This territorial vulnerability is considered at different spatial scales, representing the interface where the competent authority (inspector, regulators, and planners) interacts with industrial operators (industrial clusters or single plants) in a decision-making chain with different levels of authority and interest.

Given that the current representation of NaTech is generally scarce in European countries, with only a few maps overlaying natural and technological hazards [44], the territorial vulnerabilities of ICIs to multiple hazards here are characterized by implementing a multi-scale spatial procedure that should be contextualized to the location of concern (Fig. 3).

This procedure, consisting of 12 steps, downscales the territorial context from a large to a local scale, depending on the interest of each specific case. Then, space-dependent analyses are developed via open data and GIS to identify susceptibilities to multiple hazards, which can be useful when associated with probabilistic data based on the historical occurrence of NaTech events. The results in each scale of interest provide a territorial vulnerability profile. This can contribute to raising the

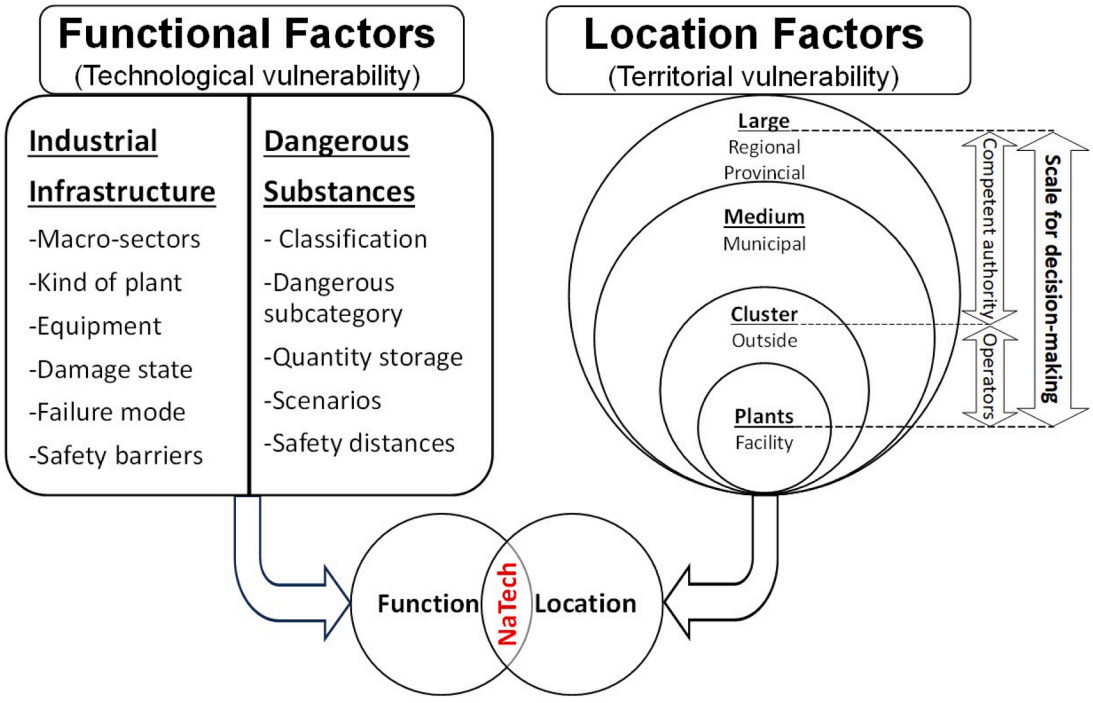

Fig. 2. Function-location approach to characterize NaTech vulnerabilities and support the decision-making process in industrial multi-hazards contexts.

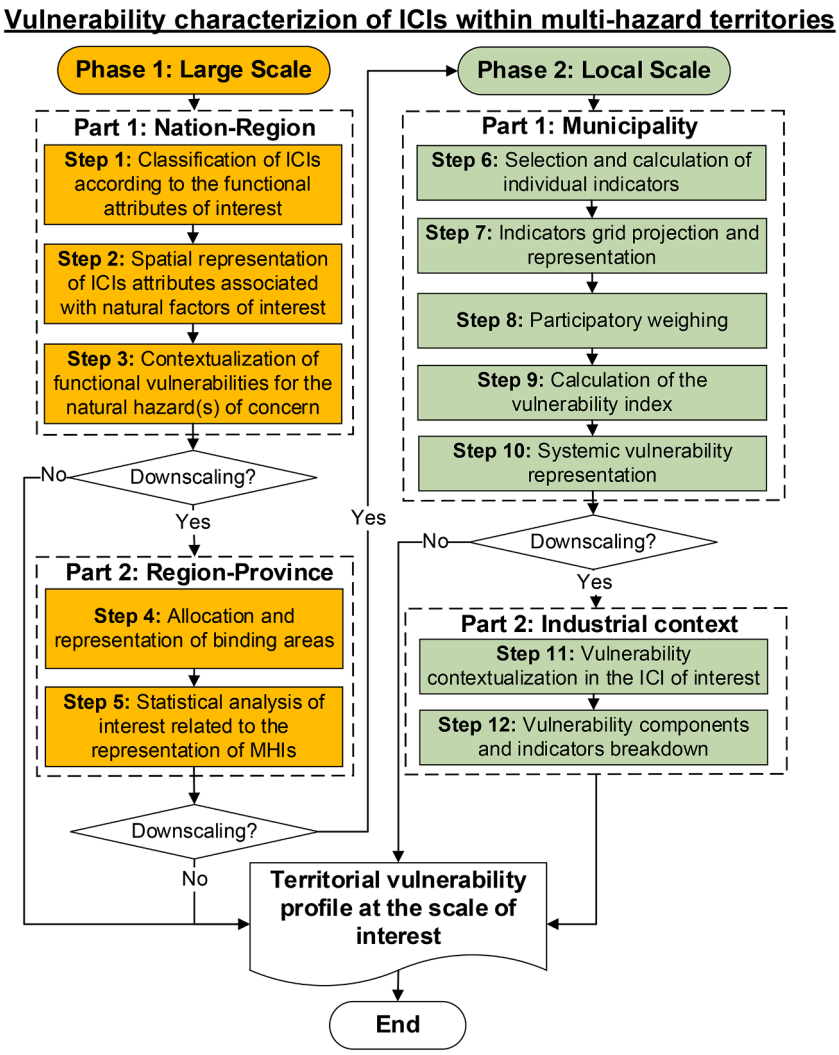

Fig. 3. Multi-scale spatial procedure to systematically characterizes the NaTech vulnerability of ICIs within multi-hazard contexts.

awareness of different levels across various interests within the decision-making chain on the control of major accidents involving hazardous substances. Furthermore, by implementing quantitative mathematical and spatial methods for vulnerability assessment, the procedure enables the calculation of indices that support decision-making with objective criteria. The next subsections will detail all the steps numbered in Fig. 3, even if, depending on the case or the scope, the procedure offers the flexibility to stop at the scale of interest obtained from the respective vulnerability profile.

3.1. Characterization of ICIs vulnerability at a large-scale

3.1.1. Phase 1-Part 1: national-regional scale

Phase 1-Part 1 represents the first half of the large-scale territorial vulnerability characterization, with a focus on national and regional profiles. It contains Steps 1, 2, and 3, which classify the ICIs according to the functional attributes of interest, followed by their representation, contextualizing the functional vulnerabilities to the natural hazards of concern.

Step 1: Classification of ICIs according to the functional attributes of interest

Since Italy was chosen as a representative European Member State due to its high number of Seveso establishments, open data within the Italian national inventory for major hazard industries (MHIs) was used for the analysis [37]. As a result, MHIs will be referred to as ICIs that are vulnerable to the potential impact of various hazards in their surroundings. The identified MHIs are grouped within the 39 categories of industrial activities used in the current Italian framework (see Legislative Decree 105/15). However, with the aim of their spatial representation, when a high concentration of points is present in the same area with a high number of diverse classifications, the overlapping data decreases the objectivity of the analysis. Therefore, it is useful to stratify and represent industrial assets via relevant attributes, such as industrial macro-sectors. Thus, the current 39 categories of industrial activities were clustered into six groups to concentrate the analysis on the principal components. The recategorization of the MHIs –considering the industrial macro-sectors to which they belong– was made according to the criteria previously defined in process-safety-related research [45, 46]. These criteria were tailored to the realities of the MHIs, where only five of the eight categories of macro-sectors matched the establishment characteristics: i) chemical and petrochemical, ii) storage and warehousing, iii) power production, iv) bioprocess, and v) manufacturing. In addition, the category "other" was retained, given the fact that within the Italian inventory, the category "other activity not specified in the list" has 85 plants, which does not allow the classification in macro-sectors. After that, the frequency of the reclassified MHIs in macro-sectors was determined by region, in association with useful public territorial data and population [47].

Step 2: Spatial representation of ICIs attributes associated with natural factors of interest

The spatialization of MHIs can begin with the representation of infrastructures as punctual elements. First, the representation of Seveso plants as punctual elements, developed by Carpanese et al. [48], was used to figure out the distribution of MHIs at the national level. After that, the macro sector distribution was represented by region at the national scale, associated with meteorological or geophysical information of interest following the function-location approach.

Regarding the natural factors of interest, Italy has hazard maps available at the national scale for various natural factors. For example, the Civil Protection Department [49] classified seismic hazards by zones, and Vanzi et al. [50] provided a synthetic formulation for this hazard and its code implications. Moreover, Claps et al. [51] created a new database of flood and catchment descriptors in Italy (FOCA), which summarizes features related to climate (discharge, rainfall, and temperature), geomorphology, soils, and land use. Additionally, the representation of landslides in Italy is given in [52,53], while insights about their susceptibility can be found in [54] and societal risk maps in Salvati et al. [55]. Furthermore, the CEI ProDis website application keeps an Italian map visualization of the number of lightning strikes per square kilometer [56].

For the sake of clarity, the case of lightning was considered a natural pilot factor to illustrate the analysis. First, the density of lightning to the ground (*Ng*) for the Italian territory was associated with the spatial distribution of MHIs at the national scale. Given that the technological vulnerabilities related to lightning-triggered NaTech events in the process industry were previously assessed in the research by Castro Rodriguez et al. [41], this data was incorporated into the analysis using the function-location approach.

Regarding *Ng*, it indicates the average yearly number of lightning strikes per square kilometer to the ground (lightning/year·km^2). After CEI Guide 81–3:1999 – "Average values of the number of lightning strikes on the ground per year and a square kilometer of the municipalities of Italy in alphabetical order" – was repealed in 2014, *Ng* started to be calculated utilizing nationwide ground lightning location networks (LLS). Geographical coordinates can be used to obtain values for specific locations from the Italian Electrotechnical Committee (CEI) through the online CEI application (CEI ProDis). Even if the document that assigned average values of *Ng* to the Italian territory [57] no longer holds normative status, it can be used as an approximation to associate the MHIs distribution with the lightning territorial vulnerability. In addition, the visualization of the number of lightning strikes per square kilometer on the CEI ProDis website application keeps an Italian map divided into three qualitative categories represented by different colors (high-red, medium-green, and low-blue). This categorized density distribution can be used to contrast the consistency of the discussions below [56].

Step 3: Contextualization of functional vulnerabilities for the natural hazard(s) of concern

For the contextualization of functional vulnerabilities, insights concerning lightning-triggered NaTech events that occurred in the process industry were introduced using a NaTech-driven dataset [58]. This dataset consisted of 689 NaTech events up until 2022 and was built via open-source industrial-accidents databases. Certain outputs were customized for this analysis, including the relative frequency of classified records for vulnerable macro-sectors affected by lightning strikes. In addition, conditional probabilities among different functional attributes of interest, such as macro-sectors, equipment, and final scenarios, were calculated. Further details regarding the methods used, the attributes, and the data analysis can be found in [41]. Subsequently, functional probabilities were used to compare two different plants belonging to the same macro-sector but hypothetically located in different regions.

3.1.2. Phase 1-Part 2: regional-provincial scale

Phase 1-Part 2 is the second half of the territorial vulnerability characterization at a large scale focused on the regional profile and zooming the scope to the provincial profile. It is composed of Step 4, which allocates binding areas to the MHIs represented as punctual elements. Subsequently, Step 5 introduces a statistical analysis of interest conducted in a GIS environment depending on the availability of data.

To do that, the Piedmont Region and Turin Province were considered to show the ICIs vulnerability at these scales, respectively. The Piedmont Region is in Northwest Italy, and Turin serves as its administrative headquarters. It is the second largest region by extension in Italy, seventh in population, and second in number of municipalities. The region is divided into provinces: Alessandria, Asti, Biella, Cuneo, Novara, Vercelli, and Verbano-Cusio-Ossola (VCO), and the metropolitan city of Turin. The concentration of many industrial activities has caused significant urban congestion, and facilities are thus concentrated in a limited, heavily populated area [59].

Step 4: Allocation and representation of binding areas

The MHIs in the region of interest were mapped using a dataset provided by the Piedmont Region,[6] where punctual elements identify the centroid of the establishments. It was then possible to define buffer zones using the GIS performing a selection by location and extracting the polygons of the industrial areas from the mosaic of the Piedmont Region.[7] The potential buffer zones represented around the MHIs followed the LUP criteria established in the local guidelines (Regional Council Resolution No 17–377, July 26, 2010) .[8] These guidelines introduce the "exclusion area" and "observation area" terms, which are subsequently detailed.

In the LUP Piedmont guidelines, the term "exclusion area" refers to the zone surrounding a production facility that must be defined for Seveso activities. The radius of this area ranges from 100 to 200 m from the facility boundary, depending on the activity risk level. For Seveso activities with higher risk, the exclusion area may extend up to 200 m for energy-related scenarios (fires and explosions) and up to 300 m for toxic incidents.

The "observation area" refers to a broader zone surrounding the facility, designed to assess and implement protective measures for the population in case of an industrial emergency. This area typically extends at least 500 m from the facility boundary and is adjusted based on the landscape, roads, and nearby settlements. The observation area does not necessarily follow a circular shape but is adapted to fit significant features at its edges. In cases involving highly toxic substances, the observation area radius can be extended to 1500 m, depending on whether the vulnerable elements are located indoors or outdoors.

Due to potential differences in the quantity and classification of hazardous substances stored at each facility (e.g., physical hazards, health hazards, and substances dangerous to the aquatic environment), multiple final scenarios can be considered, such as toxic releases, energy-related incidents, and environmental pollution. However, since the available dataset does not specify the types or quantities of hazardous substances stored, different distances were applied around the facility centroids to demonstrate the applicability of the method. Specifically, exclusion areas were set at 100 and 300 m, while observation areas were set at 500, 1000, and 1500 m, according to the extreme values for the intervals defined in the LUP Piedmont guidelines for both previously discussed concepts.

Importantly, in the presence of further data, the place-based methodology described here is compatible with other specific methodologies to determine safety distances, such as the Shortcut Method, described in Annex 6 of the Directive of the Minister for Civil Protection and Sea Policies of December 7, 2022, Part 1. This expeditious method provides a quick way to define damage and attention zones and estimate the

[6] Regione Piemonte. Dati Piemonte. https://www.dati.piemonte.it/#/home

[7] Piedmont Geoportal https://www.geoportale.piemonte.it/cms

[8] Regional Council Resolution No. 17-377, July 26, 2010, "Approval of Guidelines for Industrial Risk Assessment in Spatial Planning – Strategic Environmental Assessment Procedure and Technical Elaboration on Major Accident Hazard." Official Bulletin of the Piedmont Region No. 31, 05/08/2010.

consequences of industrial scenarios.

Step 5: Statistical analysis of interest related to the representation of MHIs

After the representation of MHIs as punctual elements and the allocation of binding areas, some statistical analyses can be introduced, depending on the availability of the data of interest. To illustrate the connection between functional and territorial factors at this scale, the safety areas previously designated were overlaid with population density data (measured as persons per hectare) based on Italian 2011 census. It was assumed that the population reported by ISTAT (National Institute of Statistics) was uniformly distributed across the areas at risk, which is a limitation conditioned by the quality of the data.

With more detailed spatial data, additional analyses could be conducted, such as assessing the population density of individual buildings or crowded centers. In addition, at this scale, it would be possible to identify not only socially vulnerable elements but also critical adjacent infrastructure that could amplify the impact of technological events. For example, identifying the number of linear access points that could be impacted, has significant implications for evacuation routes and the arrival of external security personnel during an emergency response.

3.2. Characterization of territorial vulnerability at the local scale

3.2.1. Phase 2-Part 1: vulnerability baseline at the municipal scale

As previously mentioned within the theoretical foundations section, even if the municipalities constitute the principal actor in the decision-making process to manage the different hazards through separate sectorial plans integrating strategies in the city plans and municipal emergency plans, the current methods overlook the multi-risk perspective. Establishing a municipal-level baseline to assess the vulnerabilities of critical infrastructures to multiple hazards in their surrounding areas can be valuable in supporting decision-making for various stakeholders. To achieve this goal, the multi-risk tool proposed by Beltramino et al. [60] to assess territorial vulnerability in a North Italian municipality was introduced as a proof of concept.

In summary, this multidisciplinary tool consists of the representation of an index of systemic vulnerability in a territory obtained through a mathematical framework. The calculation includes the integration of multiple predefined indicators clustered into three factors, namely, sensitivity (S), pressure (P), and hazard (H), normalized and weighted according to a participatory procedure. It not only enables the estimation of various stressors and hazards based on the vulnerable elements present at the location of interest but also allows stakeholders to assign a coefficient of relevance to the associated pressures and hazards. In addition, the mathematical equation for the estimation of systemic vulnerability considers dynamic factors for both the impact of climate change and the temporal character of the pressures. The vulnerability characterization of the tool proposed by Beltramino et al. [60] is achieved through the operations depicted in Fig. 4, which are further detailed in Steps 6, 7, 8, 9, and 10.

Step 6: Selection and calculation of individual indicators

The cornerstone of the introduced tool lies in the selection of a set of sensitivity, pressure, and hazard indicators, which are subsequently calculated using a GIS environment. These indicators were selected after a workshop involving the territorial stakeholders from the territory of interest and a multi-disciplinary research team, considering the principal spatial government plans and territorial instruments and highlighting the municipality specificities. Importantly, this methodology is open to incorporating new indicators that match sensitive elements of interest.

The definition and calculation of the indicators are the most time-consuming steps of the tool used. Each of the 21 indicators selected has followed a process of data collection, calculation, and validation in a GIS environment. For consistency, original acronyms (in Italian) were retained as in the original work.

Fig. 5 shows the set of sensitivity indicators grouped into three components (Environment and Landscape—A; Building, Heritage, and Infrastructures—B; Economy and Population—C). Beltramino et al. [60] understood sensitivity as the physical predispositions of human beings, infrastructure, and the environment to be affected by a dangerous phenomenon.

Regarding the dangerous phenomena, Fig. 6 shows the pressure and hazard indicators contextualized to the municipal case study. Pressures were considered to be linear and predictable trends that affect the system, gradually altering its condition [30]. On the other hand, the concept of multi-hazards was addressed as a combination of two or more threat factors manifested in an isolated, simultaneous, or chain reaction to produce a trigger event of a disaster, where hazardous events can be a single or more natural factor [13]. The source of the data, the description, and the calculation of each indicator can be found in previous research [60].

Step 7: Indicators grid projection and representation

The individual indicators were projected onto a grid of homogeneous cells (200 × 200 m), which covered the municipality. For their attribution to the grid, spatial join operations through a specific field identifier (FID) were assigned to each cell in the GIS environment, normalizing the values to obtain a standard metric belonging to the [0,1] interval, where 1 represents critical vulnerability.

Depending on the geometry of the input data (point, line, or polygon), the attribution of the values obtained for each indicator to the grid was carried out according to five criteria: (i) point count (Cultural heritage consistency—B1, Floods—ALA), (ii) sum of the point values (Energy consumption intensity—A3, Renewable Energy Sources (RES) energy self-sufficiency—B3, Earthquakes—SIS), (iii) weighted sum of linear (Road infrastructure density—B5) or areal elements (Landscape sensibility—A1, Ecological quality—A2, Building construction characteristics—B2, Communication infrastructure density—B4, Density of

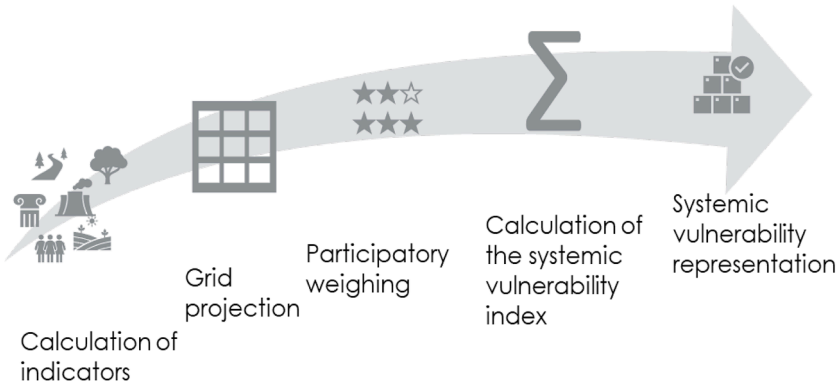

Fig. 4. Steps to characterize territorial vulnerability at the municipal scale. Source: [61].

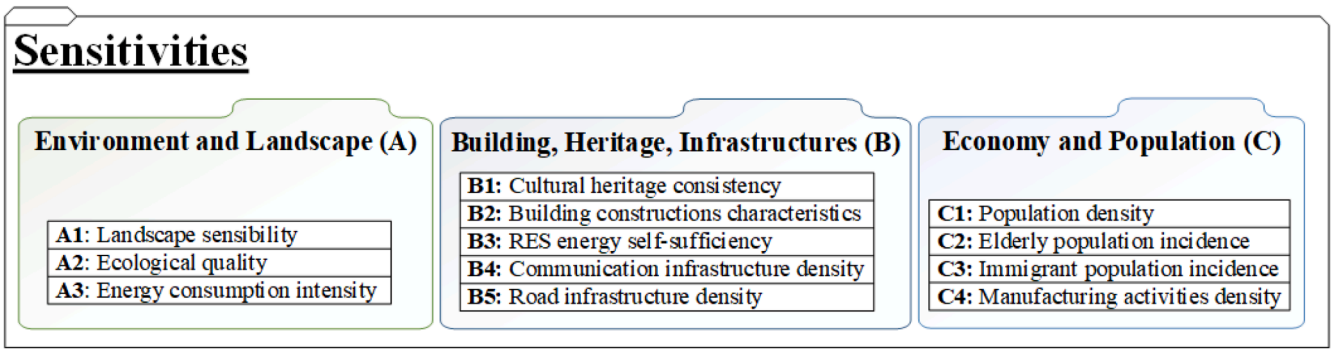

Fig. 5. Set of indicators of sensitivity divided by components to characterize territorial vulnerability at the municipal scale.
Source: modified from [60].

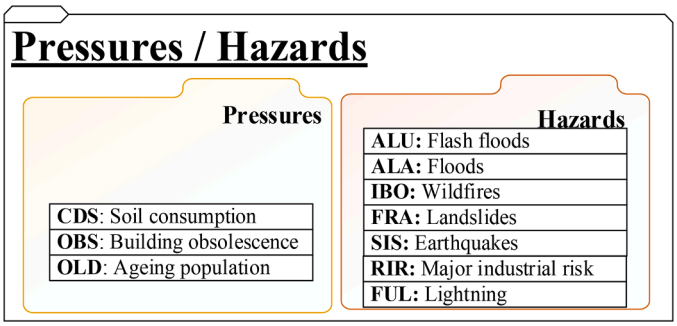

Fig. 6. Set of indicators of pressures and hazards used to characterize territorial vulnerability at the municipal scale.
Source: modified from [60].

productive activities—C4, Soil consumption—CDS, Building obsolescence—OBS, Wildfires—IBO, Lands slides—FRA), (iv) average value of areas within the cell (Population density—C1, Elderly component—C2, Immigrant component—C3, Aging population—OLD) and (v) intersection between input polygons and each cell (Flash floods—ALU, Major industrial risk—RIR). The values for each indicator and the cells for the territory meet in a table with 2550 rows (FID) and 21 columns (individual indicators).

Step 8: Participatory weighing

In Fig. 7, the relationships between each indicator of sensitivity (see Fig. 5) and each indicator of pressures and hazards (see Fig. 6) are represented within the second and third levels of the hierarchical network. Each member of a multidisciplinary team individually voted on these interactions via a crossing matrix, and the arranged mean value was assigned as shown in Fig. 8.

The weights assigned to each interaction between a sensitivity indicator and pressures or hazards were used to calculate a unique systemic vulnerability index. This index, located at the top of the hierarchical network in Fig. 7, was obtained by substituting the interaction weights into the mathematical framework outlined in the next section.

Step 9: Calculation of the systemic vulnerability index

The systemic vulnerability index is defined through the mathematical framework described in [60]. The development of equations is restated below for a better understanding.

First, for each component of the sensitivities (component A is used as an example), one can calculate the normalized index of pressures, $I_{PR(A)}$, for a single cell via Eq. (1).

$$I_{PR(A)} = \frac{1}{m_A n} \cdot \sum_{i=1}^{m_A} \sum_{j=1}^{n} K_{ij}(t) \cdot S_i \cdot b_{ij} \cdot PR_j \quad (1)$$

where,

n: number of pressures.

m_A: number of sensitivities within component A.

$K_{ij}(t)$: a factor that depends on the temporal nature of the pressure j on sensitivity i (the equation should be evaluated at two different moments—initial time t_0 and final time t_1—for the present case, the simplification $K_{ij}(t_1\text{-}t_0)=1$) was assumed).

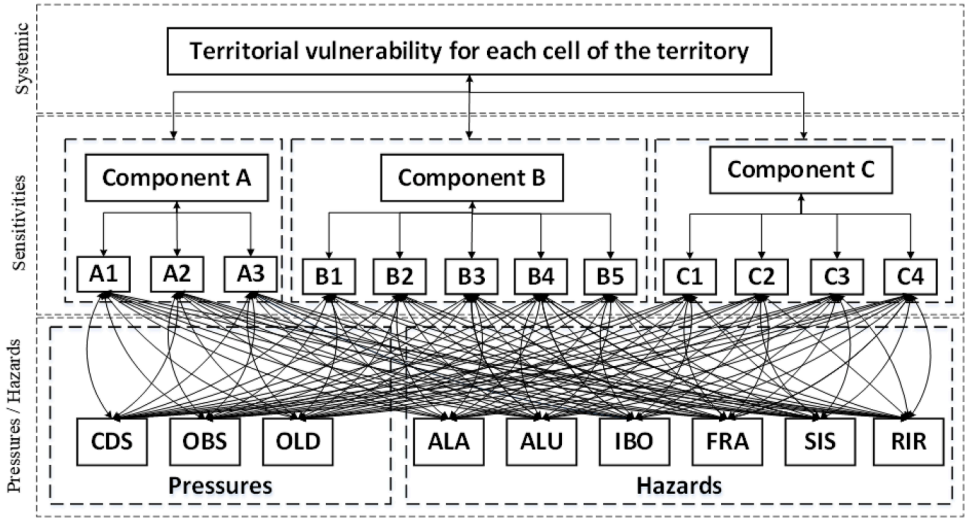

Fig. 7. A hierarchical network of three levels for territorial systemic vulnerability characterization at the municipal scale.

Components	Sensitivities	Pressures			Hazards					
		CDS	OBS	OLD	ALU	ALA	IBO	FRA	SIS	RIR
A. Environment and Landscape	A.1 Landscape sensibility	0.83	0.42	0.03	0.64	0.53	0.81	0.78	0.25	0.42
	A.2 Ecological quality	0.78	0.28	0.06	0.47	0.33	0.67	0.50	0.19	0.56
	A3 Energy consumption intensity	0.61	0.75	0.44	0.19	0.17	0.17	0.22	0.17	0.33
B. Building, Heritage, and Infrastructures	B.1 Cultural heritage consistency	0.25	0.53	0.14	0.69	0.72	0.69	0.56	0.81	0.36
	B.2 Building construction characteristics	0.28	0.92	0.19	0.39	0.47	0.36	0.44	0.69	0.31
	B.3 RES energy self-sufficiency	0.28	0.67	0.28	0.19	0.17	0.19	0.11	0.11	0.25
	B.4 Communication infrastructure density	0.50	0.39	0.22	0.67	0.56	0.47	0.53	0.47	0.44
	B.5 Road infrastructure density	0.72	0.31	0.11	0.81	0.78	0.53	0.75	0.81	0.61
C. Economy and Population	C.1 Population density	0.67	0.56	0.53	0.75	0.72	0.61	0.67	0.78	0.75
	C.2 Elderly component	0.19	0.39	0.97	0.50	0.44	0.36	0.39	0.56	0.58
	C.3 Immigrant Component	0.17	0.25	0.25	0.17	0.22	0.17	0.17	0.28	0.28
	C.4 Density of productive activities	0.56	0.44	0.17	0.86	0.78	0.64	0.61	0.83	0.94

Fig. 8. Matrix of indicators weighted through a participatory approach: grey-negligible [0, 0.15), green-low [0.15, 0.45), yellow-medium [0.45, 0.7), and red-strong [0.7, 1].
Source: modified from [60].

S_i: indicator of sensitivity i in the specific cell.

b_{ij}: indicator that describes the link between the sensitivity i and the pressure j.

PR_j: indicator of pressure j in the specific cell.

It is important to mention that the previous sum is divided by $m_A n$ to normalize the index. This means that the resulting quantity will have values between 0 and 1. Moreover, the relationship between each pressure and each sensitivity is regulated by the weighting coefficient b_{ij} (see Step 8).

Similarly, the normalized index of hazard $I_{HZ(A)}$ on a single cell can be calculated by adding together the impacts of each hazard on each sensitivity of component A (see Eq. (2)).

$$I_{HZ(A)} = \frac{1}{m_A p} \cdot \sum_{i=1}^{m_A} \sum_{k=1}^{p} CC(t)_k \cdot S_i \cdot b_{ik} \cdot HZ_k \tag{2}$$

where,

p: number of hazards.

m_A: number of sensitivities in component A.

$CC(t)_k$: a factor that expresses the impact of climate change related to hazard k (for the present case, the simplification that assumed $CC(t)_k = 1$ was considered).

S_i: indicator of sensitivity i in the specific cell.

b_{ik}: an indicator that describes the link between the sensitivity i and the hazard k.

HZ_k: indicator of hazard k in the specific cell.

Analogous to the case of pressures, the hazard index is divided by $m_A p$ to normalize it.

With respect to the other sensitivity components (B and C in this study instance, although there may be more components), the indices $I_{HZ(B)}$, $I_{HZ(C)}$, and $I_{PR(B)}$, $I_{PR(C)}$ respectively, can be calculated in a similar way (see Eqs. (1) and (2)).

Afterwards, the overall pressure index for each cell I_{PR} can be calculated by adding together the indices associated with each component of the sensitivity (A, B, and C). This sum can be weighted if the stakeholders want to assign levels of importance to the individual components of sensitivity (see Eq. (3)).

$$I_{PR} = \sum_{w=1}^{W} B_w \cdot I_{PR(w)} \tag{3}$$

where,

w: number of sensitivity components ($W = 3$ for this case: A, B, C).

B_w: weights assigned to every single component of sensitivity. ($B_w \in [0,1]$, in the present case study the three components of the sensitivity were given the same weight; then, $B_A = B_B = B_C = 1/3$).

The overall hazard index I_{HZ} is calculated similarly, as shown in Eq. (4).

$$I_{HZ} = \sum_{w=1}^{W} B_w \cdot I_{HZ(w)} \tag{4}$$

To summarize, the previous equations can be combined and generalized into Eqs. (5) and (6), respectively. This enables the independent evaluation of both indices (I_{PR}, I_{HZ}) for each cell.

$$I_{PR} = \sum_{w=1}^{W} \frac{B_w}{m_w n} \cdot \sum_{i=1}^{m_w} \sum_{j=1}^{n} K_{ij}(t) \cdot S_i \cdot b_{ij} \cdot PR_j \tag{5}$$

and,

$$I_{HZ} = \sum_{w=1}^{W} \frac{B_w}{m_w p} \cdot \sum_{i=1}^{m_w} \sum_{k=1}^{p} CC(t)_k \cdot S_i \cdot b_{ik} \cdot HZ_k \tag{6}$$

where,

m_w: number of sensitivities in component w.

The remaining terms keep their previously defined definitions.

Finally, a systemic vulnerability index is derived for each cell by adding up the two overall indices outlined in Eqs. (5) and (6). Once again, this total is a weighted sum, which means that it considers the possibility of assigning differing levels of relevance to pressures and/or hazards, assuming values in [0, 1]. Eq. (7) allows the computation of the systemic vulnerability index in each territorial cell.

$$I_V = \alpha \cdot I_{PR} + (1 - \alpha) \cdot I_{HZ} \tag{7}$$

where,

α: coefficient of "interest" in pressures/hazards ($\alpha \in [0,1]$).

The value of α ranges from 0 to 1, where α=0 means that the index only examines the hazards, while α=1 means that the index only considers the pressures. In this study, α= ½ was used.

Step 10: Systemic vulnerability representation

The main result of this spatial method is a systemic vulnerability map. This map serves as a municipal baseline for the set of indicators that are layered on top of each other via the mathematical framework described in Step 9 and the weights introduced in Step 8. Finally, detailed color-shaded vulnerability intervals are represented via a four-category ordinal scale (low-green, moderate-yellow, high-orange, and critical-red), which is useful to show systemic vulnerability in a way that can be easy to understand for decision-makers.

3.2.2. Phase 2-Part 2: industrial context scale

The bidirectional connections within the hierarchical network in Fig. 7 enable analysis at the level of nested components and indicators. This second part of the local scale, divided into Steps 11 and 12, allows for tailored vulnerability assessments targeting specific local territorial sectors. By focusing on a reduced scale, the analysis can concentrate on the territorial context surrounding critical industrial infrastructures (or clusters of them) and their nearby areas. Additionally, the projected safety distances for potentially impacted zones (as outlined in Step 4) provide valuable information to support a comprehensive evaluation of the technical and external factors at the plant level.

Step 11: ICI contextualization: The energetic critical infrastructure case study

The industrial plant used here as a case study corresponds with a thermoelectric plant clustered in the macro-sector "power production." Additionally, according to Directive (EU) 2022/2557, the establishment is classified as a critical energy infrastructure, as its primary activity is producing energy through the combustion of hydrocarbons. The plant unitary operations are both chemical and physical. The activities also include auxiliary technical systems necessary for production plant operation, such as compressed air, treated wastewater, steam production, and warehousing. Within all the processes and functions of the plant, the following items were identified: atmospheric storage tanks, tall structures such as chimneys and process columns and equipment, heat exchangers, complex systems of pipelines, complex electrical networks, water treatment components, and storage of raw materials (see Fig. 9).

The industrial area under analysis covers approximately 280 hectares and is divided into 70 uniform and mutually exclusive cells, each measuring 200 × 200 m (see Step 7). This area includes the industrial plant and its surroundings. The contextualization involves assessing the number of cells in each vulnerability category (see Step 10) to achieve a comprehensive multi-risk evaluation of the selected territory.

Step 12: Vulnerability components and indicators breakdown

To understand the extent to which each indicator contributes to the observed systemic vulnerability pattern, an analysis of sensitivity components was first conducted to identify the critical indicator. Next, a breakdown of this component was performed using the hazard indicators nested in the model, isolating their influence on the specific vulnerability.

4. Results and discussion

The results obtained from implementing the methodological framework are presented in three main subsections. The discussion first addresses the key findings and limitations of Phase 1-Part 1 and Phase 1-Part 2 (large-scale analysis). The analysis of local-scale vulnerability is then presented together for Phase 2-Part 1 and Phase 2-Part 2. Here, the focus is on the industrial context since the municipal-scale results were previously detailed in [60].

4.1. Characterization of ICIs vulnerability at large scale (national-regional): the Italian case

Table 1 shows the 978 MHIs in each Italian region after their reclassification into six macro-sectors. In addition, the final two columns present public data to contrast both datasets [47].

A higher level of industrialization can be seen in Lombardy (Lombardia), which emerges as the foremost region with 250 establishments, followed by significant contributions from Veneto (88), Emilia-Romagna (84), and Piedmont (Piemonte) (81). Interestingly, all of these regions are located in the north of the country. In contrast in the south, the only highly industrialized region is in Campania, with 78 establishments.

The data for MHIs from Table 1 is represented spatially in Fig. 10, alongside relevant hazard maps.

Fig. 10(a) merely offers a visual representation of known data coherent with previous reports [63]. However, it is noteworthy that the

Fig. 9. Satellite view of the critical energy infrastructure used as a case study. Source: modified from [61].

Table 1
Distribution of ICIs grouped by industrial macro-sector through Italian regions, with their territorial extension and population density.

Region	Chemical & Petrochemical	Storage & Warehousing	Manufacturing	Power Production	Bioprocesses	Others	Territorial extension (km^2)	Population density (inhabitant/km^2)
Abruzzo	5	8	2	0	0	8	10,832	121
Basilicata	5	3	0	0	0	2	10,063	57
Calabria	6	9	2	1	0	0	15,222	129
Campania	40	21	8	0	0	9	13,671	422
Emilia-Romagna	43	21	5	0	6	9	22,453	193
Friuli-V.G.	11	10	5	0	0	3	7924	155
Lazio	17	20	10	0	2	7	17,232	319
Liguria	6	17	2	0	0	5	5416	290
Lombardia	124	58	41	1	1	25	23,864	407
Marche	7	4	5	0	0	1	9401	164
Molise	6	1	0	0	0	0	4461	70
Piemonte	40	24	4	0	0	13	25,387	172
Puglia	10	12	5	1	0	1	19,541	207
Sardegna	11	13	7	1	0	2	24,100	68
Sicilia	19	25	2	8	1	5	25,832	194
Toscana	20	22	8	0	0	5	22,987	160
Trentino-A.A.	2	6	2	0	0	1	13,606	76
Umbria	3	5	5	0	0	0	8464	104
Valle d'Aosta	2	2	1	0	0	0	3261	39
Veneto	33	32	20	0	0	3	18,345	264

macro-sector pie charts [Fig. 10(b)] predominantly depict the "Chemical and Petrochemical," "Storage and Warehousing" and "Manufacturing" macro-sectors, with values up to 85 % of all critical MHIs in Italy.

Using the example of the lightning phenomenon and comparing the previously discussed spatial distribution with the information in Fig. 10 (c), it seems evident how almost all regions with a high or very high quantity of establishments (except for Emilia-Romagna), correspond to zones that contain medium (green), or high (yellow or red) *Ng*. On the other hand, there are regions with a medium or medium-low quantity of establishments that fall under zones with significant *Ng*, such as Friuli-Venezia Giulia, Liguria, and Lazio. Therefore, it is important to consider not only the meteorological data but also the total number of establishments and their spatial density in the region under concern. The density is influenced by factors such as the geographical extent of the territory and the eventual clustering of establishments in particular zones. For example, although Liguria has 30 establishments, approximately the same as Friuli-Venezia Giulia (29), and both are in a zone with similar *Ng* values, the likelihood of a lightning strike affecting one plant in Liguria should be higher than that in Friuli-Venezia Giulia, given that the territorial extension of Liguria is just 0.68 % of the extension of Friuli-Venezia Giulia. Furthermore, the population density that might be impacted in the case of major accidents in Liguria is 1.87 higher than that of Friuli-Venezia Giulia. Hence, it is clear that priorities should be introduced for each region according to its specific natural hazard characteristics.

Further comparisons using the lighting factor can be developed among other regions, stressing the data in Table 1 and Fig. 10(a), (b), and (c). Similarly, the discussion can be enhanced to other natural factors including the information in Fig. 10(d), (e), and (f). For the sake of conciseness and given the availability of probabilistic data from previous research [41,58], only lightning-triggered NaTech events are used as illustrative examples of natural hazards. Discussions involving other factors are proposed for future research.

The Pareto diagram in Fig. 11 shows macro-sector vulnerability, which is based on the above analysis of recorded events caused by lightning strikes in the process industry.

Notably, "Chemical & Petrochemical" (yellow) and "Storage and Warehousing" (black) account for up to 60 % of the registered lightning-triggered NaTech events worldwide in the process industry. Furthermore, if "Manufacturing" (blue) is added, these three sectors account for just under 3/4 of the analyzed NaTech events. Fig. 11 and Fig. 10(b) exhibit distinct similarities, as they both display the same macro-sector categories that are prevalent in the Italian geographical distribution of MHIs and are also the most susceptible to lightning strikes. Since these links are clearly evident, much more attention is required to enhance preparedness for lightning strikes.

The theoretical aspects of preparedness, discussed in Section 2.1, highlight two principal strategies. The first is the importance of enhancing the robustness of industrial equipment to lightning impacts, and the second is the value of strengthening the implementation of safety barriers to mitigate the expected final scenarios.

Table 2 shows the conditional probabilities for categories of vulnerable equipment given the most frequent macro-sectors affected by lightning impacts, while Table 3 illustrates further interplays between the probabilities of the final scenarios for the two most critical equipment categories. These probabilities were previously calculated [62] using a lightning-triggered NaTech-driven dataset of 689 records that can be consulted in an open repository [58]. These findings can be valuable for engineers and technicians involved in the design, evaluation, and inspection of lightning protection systems.

Table 2 shows that "storage equipment" and "electric equipment and electronic devices" are the most susceptible industrial items to lightning strikes in both critical macro-sectors. In Table 3, "fire" is the most likely outcome for storage equipment in the case of lightning strikes, accounting for 49 % of the known records. This phenomenon can be explained by the energetic charge inherent to the flash directly impacting the structure, which may ignite stored flammable material [43]. This probability of fire is consistent with reported data for ignition scenarios resulting from lightning-induced events in previous research [46]. The same authors highlighted release with no further consequences (R-NFC) as the most common scenario triggered by all NaTech events, with 45 %, which is consistent with the value obtained for the "Electric & Electronic" category (52). The disruptions caused by failures in electric equipment or electronic devices are often involved in the indirect pathway of the development of NaTech. This means that the failures are generated by overloads caused by flashes to the lines connected to the structure or near them. Consequently, the disruptions involve utilities or impairments that degrade the system performance or impede failure mitigation but do not directly cause the loss of containment of dangerous substances.

On the other hand, whereas functional factors are used to evaluate quantitative industrial contexts, geographical issues are frequently ignored or treated as less important. For example, on the historical data of NaTech events caused by lightning, it can be seen that two

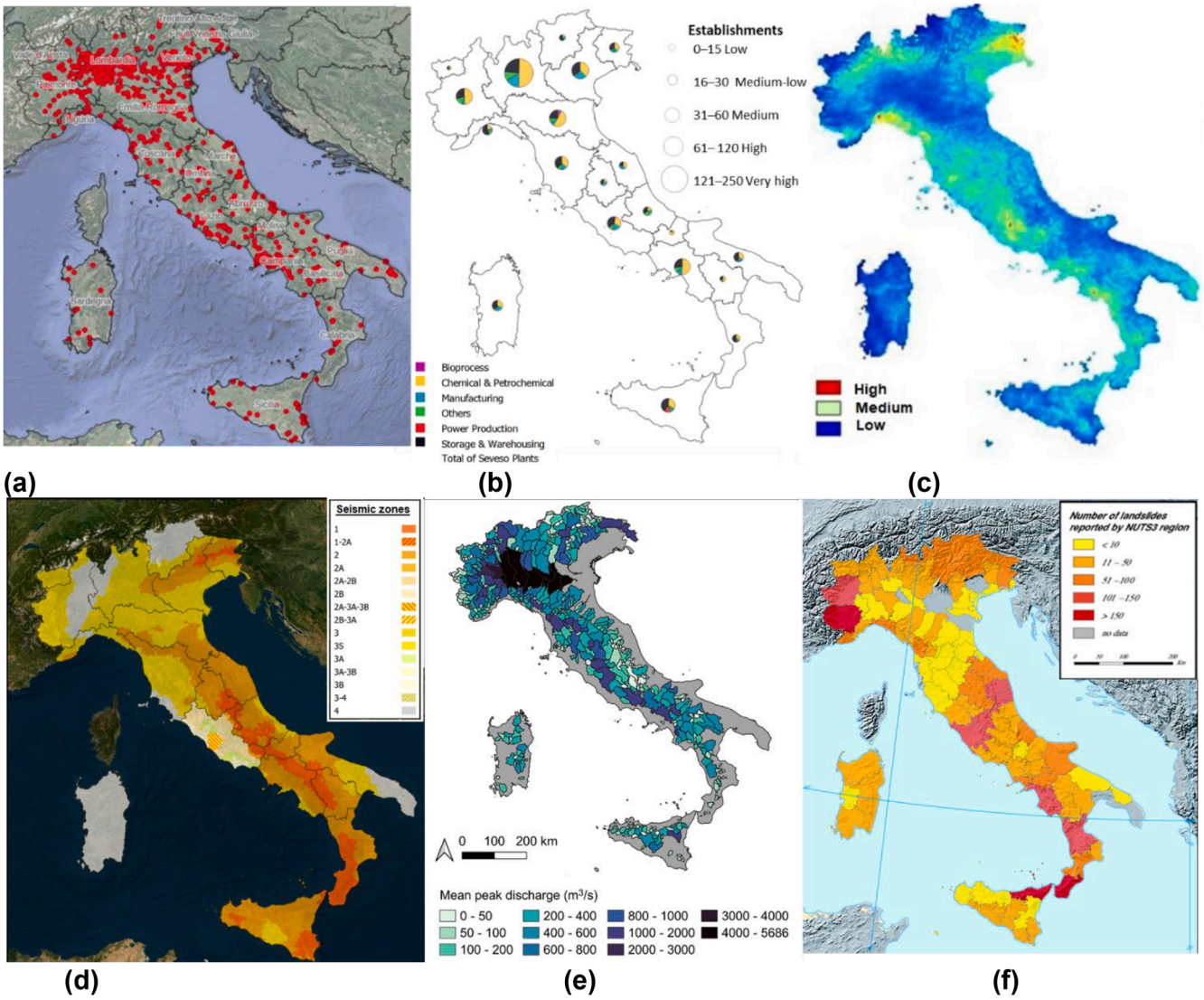

Fig. 10. Spatial representation of Italian MHIs attributes with meteorological and geophysical information: (a) Punctual representation of MHIs. Source: [48]; (b) Pie-charts for macro-sectors by region. Source: [62]; (c) Ceraunic density of lightning to the ground (lightning/year·km^2). Source: [56]–Reprinted from the CEI ProDis online application with CEI Technical Directorate approval–; (d) Seismic classification in Italy as of March 31, 2023. Source: [49]; (e) Rainfalls: spatial distributions of the mean peak discharge. Source: [51]; f) Number of landslides reported in Italy (1998–2001). Source: [52].

hypothetical companies in the "Chemical and Petrochemical" macro-sector—Plant A from Liguria (with 30 companies per region) and Plant B from Apulia (Puglia) (with 29 companies per region)—will have the same conditional probability of equipment being affected by lightning, for example, the "Storage Equipment" sub-category (0.46, according to Table 2). However, because Apulia has a lower *Ng* [see Fig. 10(c)], the risk of a lightning strike clearly differs between Apulia and Liguria but is not taken into account. Furthermore, the Apulia extension is 3.6 times greater than that of Liguria, resulting in different densities of establishments per area for each region (0.0055 establishments/km^2 in Liguria, whereas Apulia presents 0.0014 establishments/km^2). Evidently, location factors influence the assessment of infrastructure susceptibility to lightning strikes between Plant A and Plant B. In our view, the function-location approach outlined here for lightning could also be applied to other natural hazards when characterizing vulnerabilities.

4.2. *Characterization of ICIs vulnerability at large scale (Region-Province): piedmont region and turin province*

Fig. 12 represents, on its right side, the system of ICIs within the Piedmont Region, which interact with each other for energy and stock and to provide their products for the development of society. In parallel, this system represents nodes that potentially threaten the environmental, social and structural elements anchored in the territory. The punctual representation of MHIs enables us to replicate, in major detail, the analysis previously discussed at the national level. On the one hand, the binding areas around the establishments represent their potential impact on the territory in the case of different technological scenarios. The superposition of the damaged areas for neighboring establishments has implications for the identification of potential domino effects. For example, moving to the zoomed quadrant concerning the Metropolitan City of Turin (left side of Fig. 12), it can be appreciated that several areas with a high concentration of establishments are superposing their damaged areas.

According to the definitions in Annex E of Legislative Decree 105/15

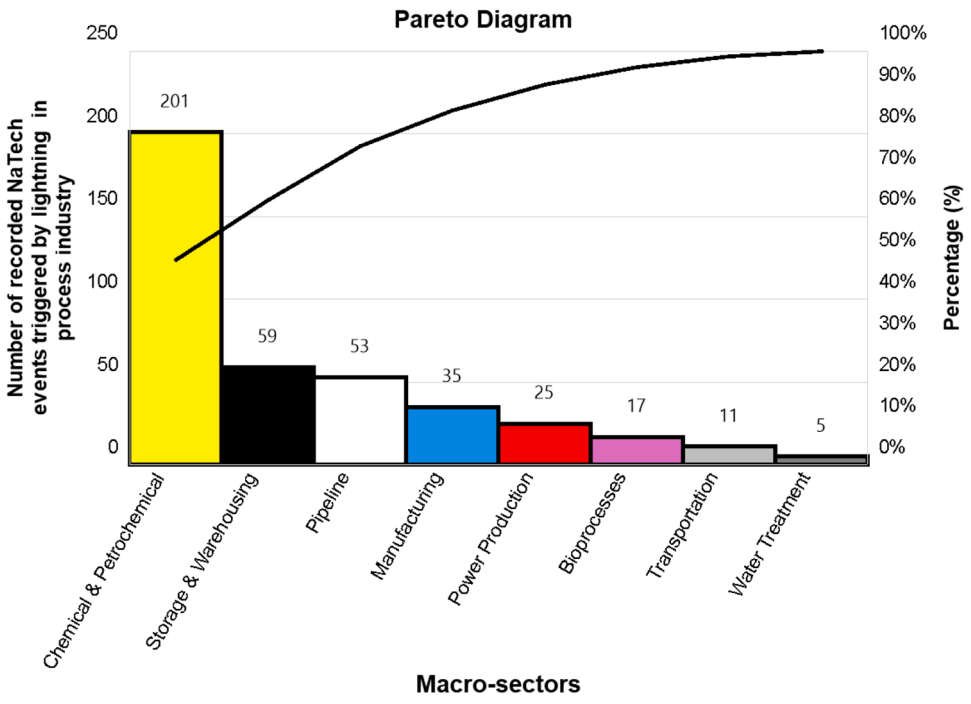

Fig. 11. Pareto diagram for macro-sector vulnerability to lightning-triggered NaTech events within the process industry. Source: [62].

Table 2
Conditional probabilities for categories of vulnerable equipment, given the most critical macro-sectors impacted by lightning within Italian MHIs. Source: [62].

Equipment	Process	Storage equipment	Pipework	Electric & Electronic	Machinery	Flares & Stakes	Other
Chemical & Petrochemical	0.08	0.46	0.03	0.32	0.07	0.02	0.03
Storage & Warehousing	0	0.79	0.02	0.11	0.05	0.01	0.01

Table 3
Conditional probabilities for technological scenarios given the failure of the vulnerable equipment to lightning strikes. Source: [62].

Equipment	Fire	Explosion	Release without consequences	Toxic gas Dispersion	Environmental contamination	Multiple scenarios
Storage Equipment	0.49	0.05	0.15	0.00	0.13	0.18
Electric & Electronic	0.08	0.01	0.52	0.02	0.32	0.05

(Parts 1 and 2), Potential Areas-RIR (RIR means "major industrial risk" in Italian) refer to locations with a high concentration of MHIs that may cause a domino effect. It means that in those areas, at least two domino groups with a distance lower than 1500 m or one domino group with three or more establishments are present. In the case of undesired technological scenarios inside an Area-RIR, it may trigger cascading and escalating events with more severe consequences affecting neighboring plants or essential infrastructure. Returning to the left side of Fig. 12, more than one Area-RIR can be identified. Consequently, according to legal policies, a Safety Study Integrated of Area (SSIA) should be carried out in these Areas-RIR, including mapping tools and thematic charts. Even though some criteria are stated within the text of the transposed legal framework, there are no references to specific spatial methods for conducting the SSIA.

Fig. 13 presents a bar graph for the density of inhabitants within the different damaged areas by province. The density of people in the Seveso exclusion areas (100 to 300 m) in the provinces of Asti, Vercelli, Cuneo, and Verbano-Cusio-Ossola (VCO) is higher than in other provinces that accumulated more Seveso installations, such as Alessandria or Turin. Moving to the experimental observation areas used (ranging from 500 to 1500 m), the same three provinces, Vercelli, Cuneo, and VCO, are confirmed as more vulnerable concerning the people inside the potential damage zones, in comparison with the metropolitan city of Turin. This issue suggests potential incompatibility with the minimum safety criteria regarding land use around Seveso establishments, particularly concerning distances, for existing plants located in populated zones.

Based on the quality of the available data, certain assumptions have been made, such as the uniform distribution of people across each buffer zone. Therefore, the results should be regarded as a preliminary assessment of people vulnerability, with further specific analyses recommended in the case of any warnings. Although this stage focuses on a large-scale analysis, a more detailed assessment was conducted to demonstrate the potential of the methodology by zooming in on one of the plants shown in the left part of Fig. 12. Fig. 14 shows the results of applying population density statistics to the volumes of individual structures while maintaining the previously established buffer zones. The building volumes were extrapolated using the official cartography of the Piedmont Region (BDTRE).

Fig. 14 clearly illustrates that the assumption of a uniform distribution of people across the damage areas is not real. Specifically, most residents are concentrated in buildings located in the southwestern part of the plant, while the northeastern area remains uninhabited. Despite

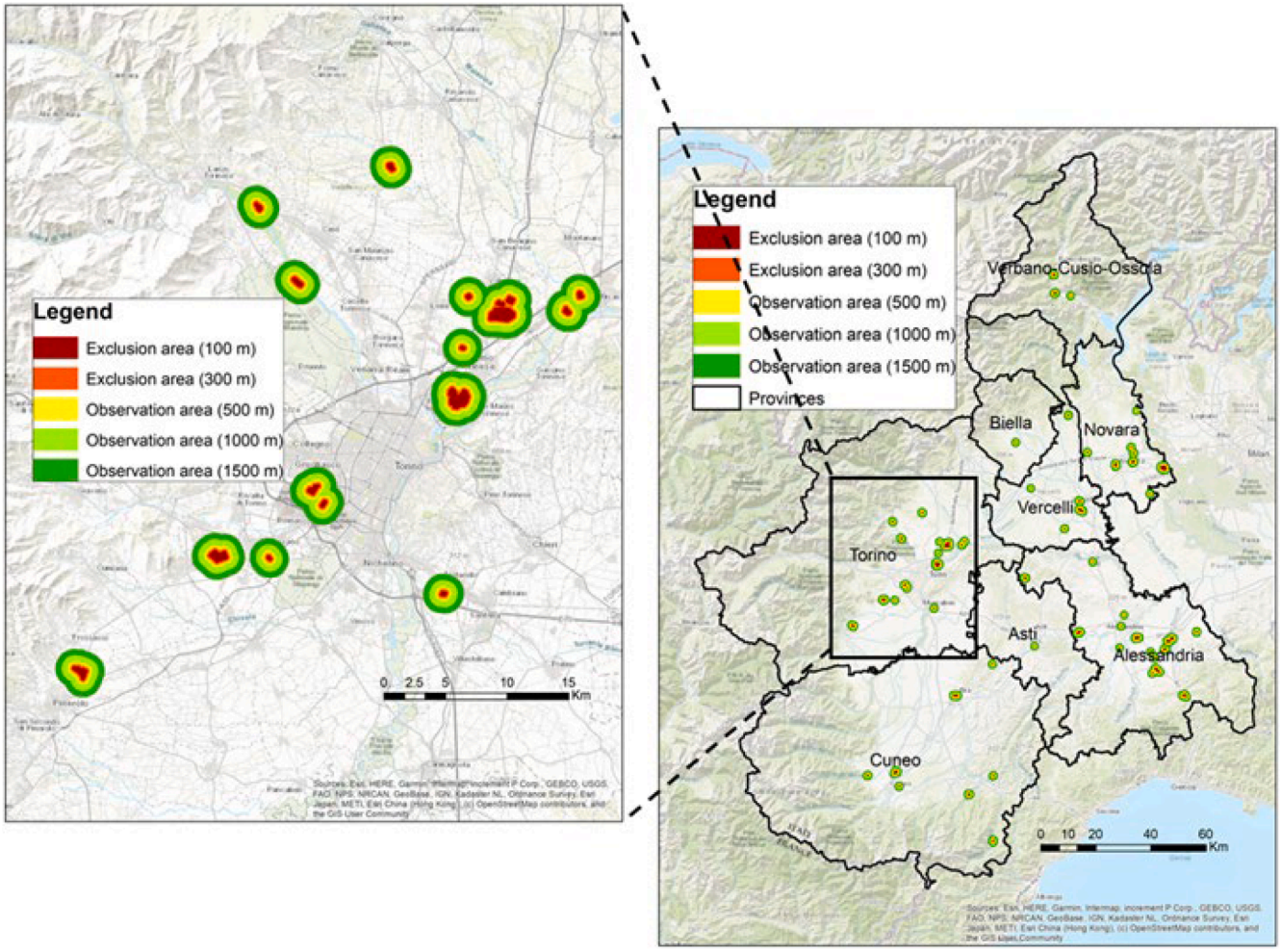

Fig. 12. Representation of Seveso establishment and binding areas in Piedmont and zoom for sector containing the establishments in the Metropolitan City of Turin. Modified from [64].

this, it is evident that the most densely populated buildings fall within the projected exclusion zones (100 m and 300 m), which is in line with the previous pattern observed at the large scale. This poses a significant risk, as these areas would contravene the regional guidelines in the event of toxic scenarios, potentially affecting a large portion of the nearby population.

4.3. Territorial vulnerability characterization at municipal scale: insights from the context around an energetic critical infrastructure contextualization

The principal output of the GIS-tool described in Step 10 of the methodological framework is shown in Fig. 15(a).

The critical susceptible areas observed at the municipal scale primarily include the historical center, industrial sectors, and densely populated regions in the North and Northwest. Other scattered locations imply punctual aspects of the territory. However, since these visualizations depend on the availability of spatial data and involve certain assumptions for calculating and spatializing the indicators, they may introduce uncertainties into the model. Therefore, meticulous validation of the model results with respect to territorial characteristics is a crucial issue. This involved both statistical and spatial verification, drawing on the expertise of planners and stakeholders in the territory of concern. Importantly, this municipal case study served as a foundation for establishing an initial baseline of systemic vulnerability. During this process, the indicators, the procedures for their calculation, and the weight matrix were also defined. More details can be found in [60]. However, depending on the necessities, it is possible to disregard, add, or refine some of the indicators used, adjusting the weight matrix to reflect the place-based characteristics.

The industrial context shown in Fig. 15(b) highlights a section of the municipality systemic vulnerability. The industrial area includes not only the space within the fence of the facility but also the surrounding neighboring territory. Additionally, the figure shows the boundaries for exclusion and observation zones, neighboring plants, and relevant urban and geographical features.

The visual field analysis of systemic vulnerability revealed the following distribution of vulnerable cells: 65 % with moderate vulnerability (yellow), 26 % with high vulnerability (orange), and 9 % with critical vulnerability (red). Notably, the critical vulnerability cells were observed in external regions just partially intersecting the observation area of 500 m. In contrast, inside the plant perimeter, over 50 % of the area is characterized by coloration, which indicates a high level of vulnerability. Furthermore, the exclusion zone partially intersects three additional high-vulnerability cells. Overall, the energetic critical infrastructure of concern seems susceptible to the external hazards in its surroundings, considering the systemic vulnerability indicator.

Since there are zones with high or critical vulnerability, the real causes must be deepened to avoid cascading events that could harm the environment, population, and infrastructure. In this regard, Fig. 16 shows a vulnerability breakdown by the components of sensitivity. Specifically, Component A has almost no susceptible cells within the

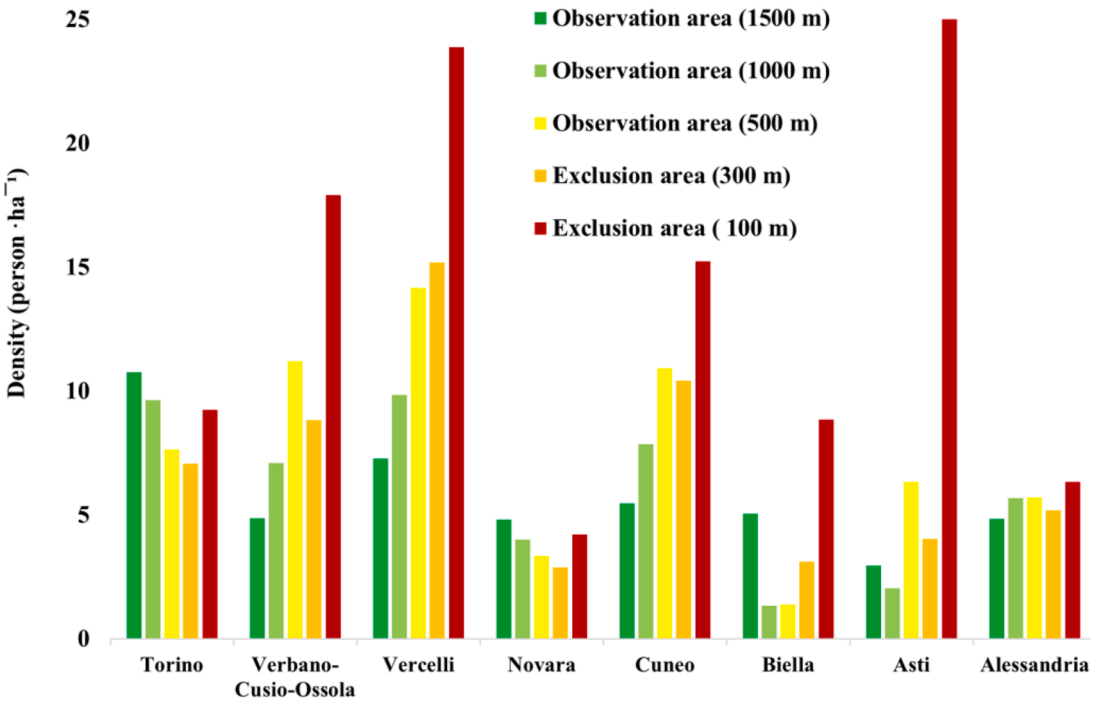

Fig. 13. Density of inhabitants (person·ha^{-1}) by province in the applied buffer zones.
Source: [64].

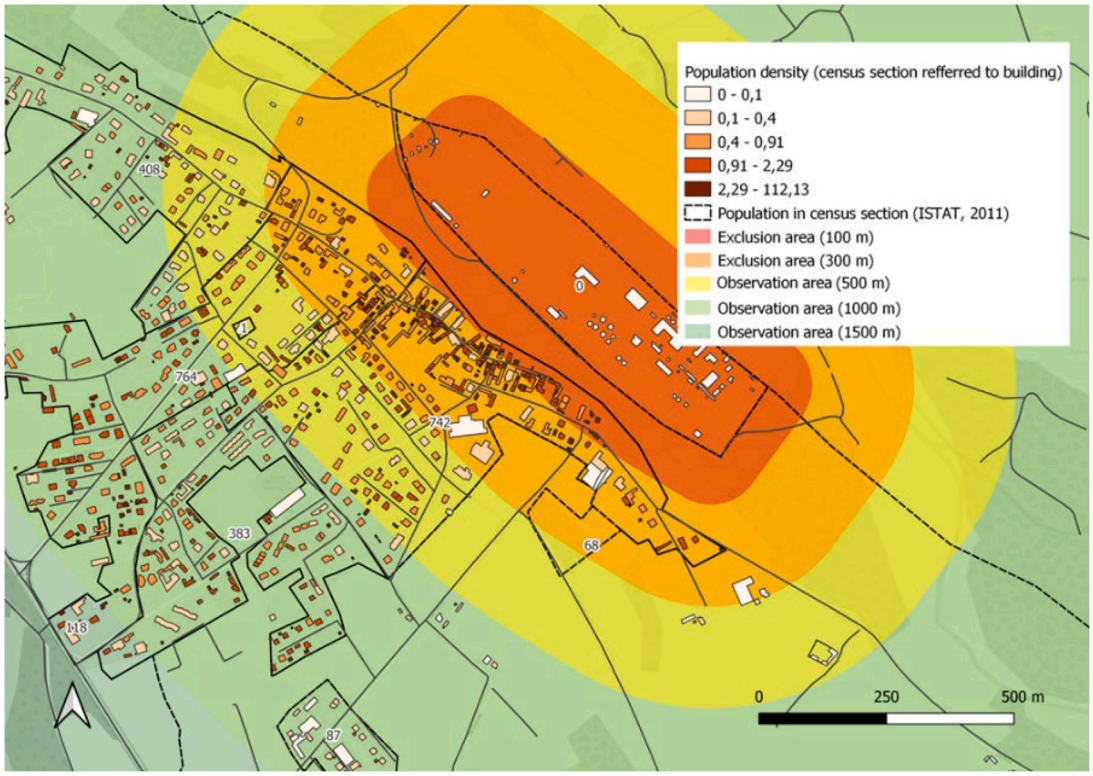

Fig. 14. Details of a chemical plant, including the allocation of the buffer zones and the statistical data of interest.
Source: [64].

industrial context under consideration. In contrast, the observed patterns for components B and C reveal cells with high and critical vulnerability. Although the study of Component C may be valuable for stakeholders, this research will focus on Component B, which shows a significant critical status and includes the infrastructural dimension.

To exemplify the multi-hazard perspective, a second breakdown at the level of hazard indicators was performed. Thus, factors with different incidences of component B sensitivity are contrasted. For example, Fig. 17 shows several natural hazards that can be disregarded in this specific case, whereas Fig. 18 illustrates critical factors.

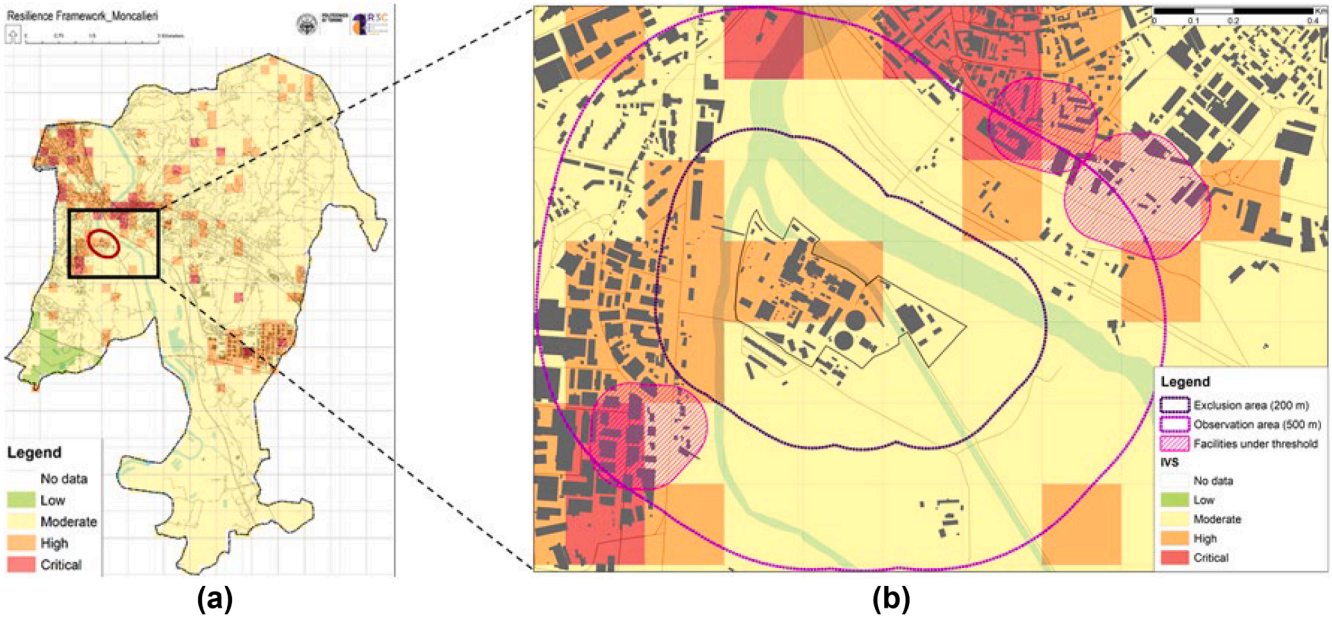

Fig. 15. (**a**) Systemic vulnerability map for the municipality case study. Source: Modified from [60]. (**b**) Systemic vulnerability for the industrial context of interest. Source: modified from [61].

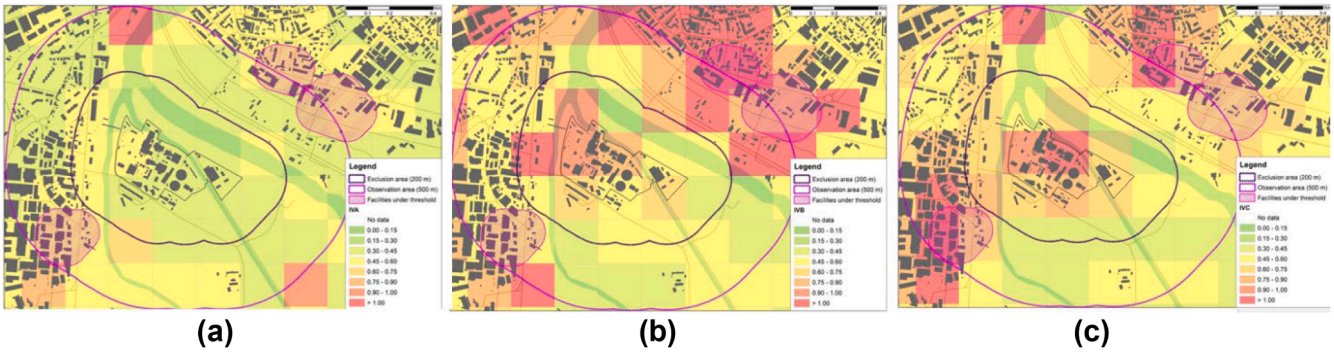

Fig. 16. Territorial vulnerability by components of sensitivity. (a) Environment and Landscape (A). (b) Building, Heritage, and Infrastructures (B). (c) Economy and Population (C).

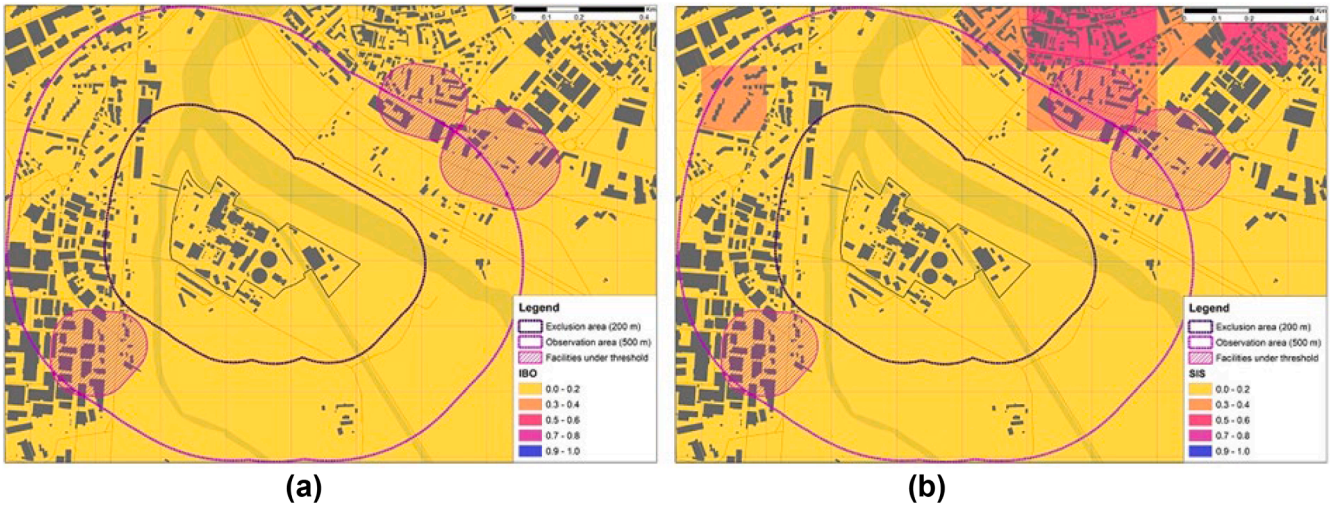

Fig. 17. Vulnerability representation of hazards not significant to the industrial context. (a) Wildfires (IBO). (b) Seismic (SIS). Source: [65].

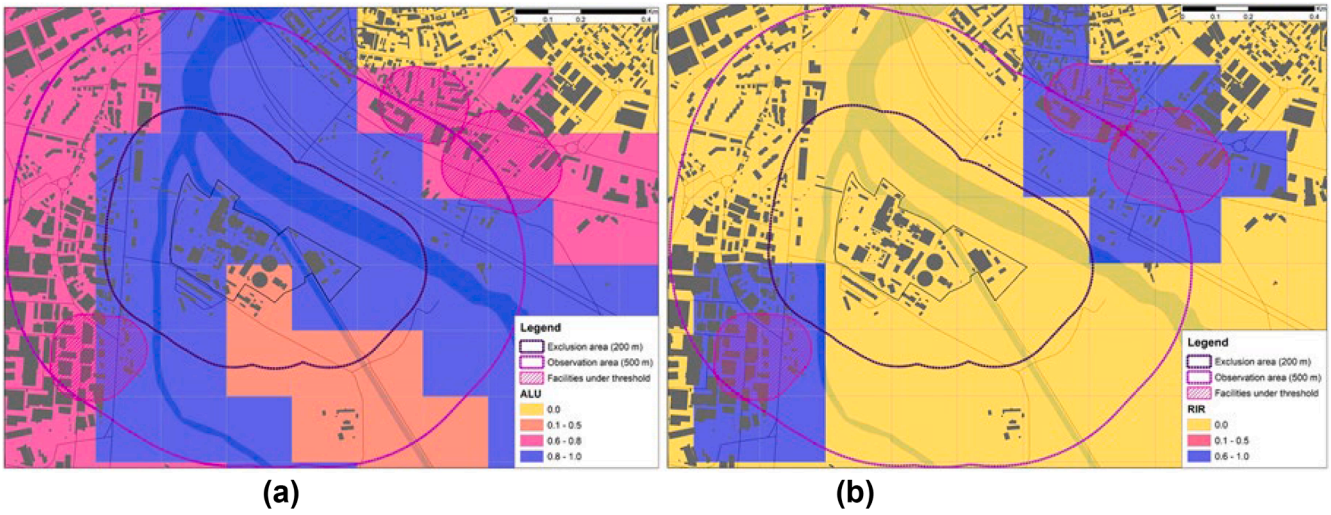

Fig. 18. Vulnerability representation of hazards significant to the industrial context. (a) Floods (ALU). (b) Industrial risk (RIR). Source: modified from [65].

From the picture above, even though earthquake and wildfire risks should not be completely ignored, the industrial context presents low vulnerability to these risks. In the case of Fig. 17(b), this visualization matches the level of danger concerning the seismic zone of concern [49].

Fig. 18(a) shows how almost all the cells in the exclusion area are very sensitive to flooding (near to 1). This includes cells that are inside the plant boundaries. The rest of the visual field in the industrial context alternates between critical and high vulnerability. Because the plant is close to the bed of a river that splits in two, the effects of this natural hazard could be evident. However, since the flood hazard may cause multiple damage modes to industrial items [66,67], then the presence of areas with nonnegligible vulnerabilities suggests that further analysis should adopt specific quantitative risk assessments to better estimate the consequences of potentially triggered NaTech scenarios.

Referring to Fig. 18(b), the cells in blue correspond with the representation of major industrial hazard vulnerability, corresponding with neighboring facilities. Analyzing the major risk hazard vulnerability layer, it is possible to identify the intersections in the potentially damaged areas of both neighboring facilities and the thermoelectric plant. Then, in cases of technological scenarios, these two-way interplays have significant implications for subsequent domino effect scenarios.

5. Conclusions

In conclusion, this research assessed the vulnerabilities of critical industrial infrastructures to multiple hazards, creating a comprehensive territorial vulnerability profile at both large and local scales via a spatial analysis method. This approach contributes the territorial vulnerability component to the introduced function-location framework, aiding in decision-making for controlling major accidents involving hazardous substances. While the methodology was tested using hazards specific to the Italian context, it has broad applicability for evaluating the vulnerability of ICIs to hazards in other regions.

At a large scale, the geographical distribution of ICIs allows for linking functional vulnerability with relevant natural factors. The methodology was illustrated using lightning as a pilot case, highlighting the complex interplay and setting the stage for further analysis with other natural hazards, in the presence of available data about NaTech occurrence. Additionally, the introduction of buffer zones around ICIs, which outline different safety areas, proved valuable for identifying populations at risk in accident-prone areas. This procedure also helps pinpoint regions with high concentrations of establishments, indicating the need for more detailed analyses at smaller scales when warnings are detected. These findings have implications for land use planning and the detection of potential domino effects, offering a quick method to identify incompatibility between existing or new projected facilities. Increased data accuracy enables the development of more comprehensive studies utilizing this approach.

At the local scale, the introduction of a previously validated GIS tool for assessing vulnerability at the municipal level serves as a proof of concept, establishing a foundation for the SSIA. The resulting vulnerability map effectively demonstrates systemic vulnerability from a multi-risk perspective, offering a comprehensive overview for decision-makers and stakeholders. This baseline provides tailored assessments for specific sectors, which is especially useful for land use planning involving not only industrial plants but also other critical infrastructures and demographic factors, both within and beyond facility boundaries. Future research should focus on integrating new sensitivity and hazard indicators into the model. Additionally, ongoing efforts are needed to operationalize the temporal dynamics of pressures and hazards, as well as their interactions, to better capture cascading effects.

The case study of an energetic critical infrastructure enabled the contextualization of systemic vulnerability at the industrial scale. The multi-risk hierarchical structure used allowed for the breakdown of the analysis into sensitivity components, identifying the specific impacts of individual hazard indicators within the contextualized framework. Notably, the “Building, Heritage, and Infrastructure” component was particularly susceptible to the hazards considered in the model, especially flooding, with neighboring industrial facilities due to the two-way interaction (impacting and being impacted).

Finally, this research provides specific methods to address the vulnerabilities of ICIs to hazards within their surroundings and help to bridge the historical gap between technical and external factors disconnect. The developed procedure enhances awareness of vulnerabilities, serving as a crucial first step toward strengthening the resilience of ICIs.

Ethics statement

This research did not involve any applicable ethics statement, and all research procedures were carried out following the requirements for ethical principles.

Funding

Part of this study was carried out within the RETURN Extended Partnership and received funding from the European Union

NextGenerationEU (National Recovery and Resilience Plan – NRRP, Mission 4, Component 2, Investment 1.3 – D.D. 1243 August 2, 2022, PE0000005).

CRediT authorship contribution statement

David Javier Castro Rodriguez: Writing – original draft, Visualization, Software, Methodology, Investigation, Conceptualization. **Antonello A. Barresi:** Writing – review & editing, Validation, Supervision, Project administration, Funding acquisition, Formal analysis, Data curation. **Micaela Demichela:** Writing – review & editing, Validation, Supervision, Methodology, Formal analysis, Conceptualization.

Declaration of competing interest

The authors declare that they have no known competing financial interests or personal relationships that could have appeared to influence the work reported in this paper. All authors declare that there are no competing interests.

Acknowledgements

Part of the methodology used in this manuscript was developed under the interdisciplinary research project "Measuring Urban Resilience," conducted by the Interdepartmental Responsible Risk Resilience Centre (R3C) at Politecnico di Torino (see http://www.r3c.polito.it). The authors also recognize the assistance of Ph.D. Simone Beltramino and Ph.D. Mattia Scalas for GIS use.

References

[1] P. Swuste, G. Reniers, Seveso inspections in the European low countries history, implementation, and effectiveness of the European Seveso directives in Belgium and The Netherlands, J. Loss. Prev. Process. Ind. 49 (2017) 68–77, https://doi.org/10.1016/j.jlp.2016.11.006. Part A.

[2] European Commission, Report from the Commission to the European Parliament and the Council on the implementation and efficient functioning of directive 2012/18/EU on the control of major-accident hazards involving dangerous substances for the period 2015-2018 (No. COM(2021) 599), 2021. Brussels, Belgium.

[3] J. Taveau, Risk assessment and land-use planning regulations in France following the AZF disaster, J. Loss. Prev. Process. Ind. 23 (6) (2010) 813–823, https://doi.org/10.1016/j.jlp.2010.04.003.

[4] E. Pilone, M. Demichela, G. Camuncoli, Seveso Directives and LUP: the mutual influence of natural and anthropic impacts, J. Loss. Prev. Process. Ind. 49 (2017) 94–102, https://doi.org/10.1016/j.jlp.2017.02.027. Part A.

[5] E. Pilone, V. Casson Moreno, V. Cozzani, M. Demichela, Climate change and NaTech events: a step towards local-scale awareness and preparedness, Saf. Sci. 139 (2021) 105264, https://doi.org/10.1016/j.ssci.2021.105264.

[6] S.P. Showalter, F.M. Myers, Natural disasters in the United States as release agents of oil, chemicals, or radiological materials between 1980 and 1989: analysis and recommendations, Risk Anal. 14 (2) (1994) 169–182, https://doi.org/10.1111/j.1539-6924.1994.tb00042.x.

[7] J. Johnston, L. Cushing, Chemical exposures, health, and environmental justice in communities living on the fenceline of industry, Curr. Environ. Health Rep. 7 (2020) 48–57, https://doi.org/10.1007/s40572-020-00263-8.

[8] G. Reniers, N. Khakzad, V. Cozzani, F. Khan, The impact of nature on chemical industrial facilities: dealing with challenges for creating resilient chemical industrial parks, J. Loss. Prev. Process. Ind. 56 (2018) 378–385, https://doi.org/10.1016/j.jlp.2018.09.010.

[9] E. Krausmann, D. Baranzini, NaTech risk reduction in the European Union, J. Risk. Res. 15 (2012) 1027–1047, https://doi.org/10.1080/13669877.2012.666761.

[10] E. Pilone, M. Demichela, A semi-quantitative methodology to evaluate the main local territorial risks and their interactions, Land Use Policy 77 (2018) 143–154, https://doi.org/10.1016/j.landusepol.2018.05.027.

[11] United Nations, 2016. Report of the open-ended intergovernmental expert working group on indicators and terminology relating to disaster risk reduction. A/71/644. Seventy-first session. Agenda item 19 (c). (p. 41). United Nations General Assembly. URL: https://www.undrr.org/publication/report-open-ended-intergovernmental-expert-working-group-indicators-and-terminology. See also Update: https://www.undrr.org/drr-glossary/terminology.

[12] Glossary, in: E. Krausmann, A.M. Cruz, E. Salzano (Eds.), NaTech Risk Assessment and Management, Elsevier, 2017, pp. 241–243, https://doi.org/10.1016/B978-0-12-803807-9.00019-X.

[13] A. Mesa-Gómez, J. Casal, F. Muñoz, Risk analysis in NaTech events: state of the art, J. Loss. Prev. Process. Ind. 64 (2020) 104071, https://doi.org/10.1016/j.jlp.2020.104071.

[14] G. Brunetta, R. Ceravolo, C.A. Barbieri, A. Borghini, F. de Carlo, A. Mela, S. Beltramo, A. Longhi, G. De Lucia, S. Ferraris, A. Pezzoli, C. Quagliolo, S. Salata, A. Voghera, Territorial resilience: toward a proactive meaning for spatial planning, Sustainability 11 (2019) 2286, https://doi.org/10.3390/su11082286.

[15] C.-H. Hung, H.-C. Hung, M.-C. Hsu, Linking the interplay of resilience, vulnerability, and adaptation to long-term changes in metropolitan spaces for climate-related disaster risk management, Clim. Risk Manag. 44 (2024) 100618, https://doi.org/10.1016/j.crm.2024.100618.

[16] S. Davoudi, E. Brooks, A. Mehmood, Evolutionary resilience and strategies for climate adaptation, Plan. Pract. Res. 28 (3) (2013) 307–322, https://doi.org/10.1080/02697459.2013.787695.

[17] E. De Rademaeker, G. Suter, H.J. Pasman, B. Fabiano, A review of the past, present and future of the European loss prevention and safety promotion in the process industries, Process Saf. Environ. Prot. 92 (4) (2014) 280–291, https://doi.org/10.1016/j.psep.2014.03.007.

[18] L.T.T. Dinh, H. Pasman, X. Gao, M.S. Mannan, Resilience engineering of industrial processes: principles and contributing factors, J. Loss. Prev. Process. Ind. 25 (2012) 233–241, https://doi.org/10.1016/j.jlp.2011.09.003.

[19] B. Fabiano, C. Vianello, A.P. Reverberi, E. Lunghi, G. Maschio, A perspective on Seveso accident based on cause-consequences analysis by three different methods, J. Loss. Prev. Process. Ind. 49 (2017) 18–35, https://doi.org/10.1016/j.jlp.2017.01.021. Part A.

[20] B. Fabiano, G. Reniers, Editorial: the Seveso disaster and its 40-year legacy to process safety, J. Loss. Prev. Process. Ind. 49 (2017) 1–4, https://doi.org/10.1016/j.jlp.2017.07.006. Part A.

[21] S. Hosseini, K. Barker, J.E. Ramirez-Marquez, A review of definitions and measures of system resilience, Reliab. Eng. Syst. Saf. 145 (2016) 47–61, https://doi.org/10.1016/j.ress.2015.08.006.

[22] S. Meerow, J.P. Newell, M. Stults, Defining urban resilience: a review, Landsc. Urban. Plan. 147 (2016) 38–49, https://doi.org/10.1016/j.landurbplan.2015.11.011.

[23] P. Jain, H.J. Pasman, S.P. Waldram, W.J. Rogers, M.S. Mannan, Did we learn about risk control since Seveso? Yes, we surely did, but is it enough? An historical brief and problem analysis, J. Loss. Prev. Process. Ind. 49 (2017) 5–17, https://doi.org/10.1016/j.jlp.2016.09.023. Part A.

[24] S. Cincotta, N. Khakzad, V. Cozzani, G. Reniers, Resilience-based optimal firefighting to prevent domino effects in process plants, J. Loss. Prev. Process. Ind. 58 (2019) 82–89, https://doi.org/10.1016/j.jlp.2019.02.004.

[25] E. Hollnagel, D.D. Woods, N. Leveson, Resilience Engineering | Concepts and Precepts, 1st ed., CRC Press Taylor & Francis Group, New York, NY, 2006.

[26] D.-H. Ham, Safety-II and resilience engineering in a nutshell: an introductory guide to their concepts and methods, Saf. Health Work 12 (2021) 10–19, https://doi.org/10.1016/j.shaw.2020.11.004.

[27] A. Wardekker, B. Wilk, V. Brown, C. Uittenbroek, H. Mees, P. Driessen, M. Wassen, A. Molenaar, J. Walda, H. Runhaar, A diagnostic tool for supporting policymaking on urban resilience, Cities 101 (2020) 102691, https://doi.org/10.1016/j.cities.2020.102691.

[28] R. Remenyte-Prescott, V. Kopustinskas (Eds.), Modelling the Resilience of Infrastructure Networks – An ESReDa Project Group Report, European Safety, Reliability & Data Association (ESReDA)., Det Norske Veritas, Norway, 2021.

[29] European Commission, Periodic reporting for period 2 - SmartResilience (Smart Resilience Indicators for Smart Critical Infrastructures) | H2020 (No. 700621), STEINBEIS EU-VRI GMBH, Germany, 2020.

[30] Intergovernmental Panel on Climate Change (Ed.), Climate change 2021 – The physical science basis. Contribution of Working Group I to the Sixth Assessment Report of the Intergovernmental Panel On Climate Change, 1st ed., Cambridge University Press, Cambridge, United Kingdom and New York, NY, USA, 2023 https://doi.org/10.1017/9781009157896.

[31] P. Amyotte, Y. Irvine, F. Khan, Chemical safety board investigation reports and the hierarchy of controls: round 2, Process Saf. Prog. 37 (2018) 459–466, https://doi.org/10.1002/prs.12009.

[32] M. Tanabe, C. Turco, A. Miyake, Management system for enhancing chances to take inherently safer design options in LNG plant projects, J. Loss. Prev. Process. Ind. 49 (2017) 120–128, https://doi.org/10.1016/j.jlp.2016.07.030.

[33] A. Misuri, G. Antonioni, V. Cozzani, Quantitative risk assessment of domino effect in NaTech scenarios triggered by lightning, J. Loss. Prev. Process. Ind. 64 (2020) 104095, https://doi.org/10.1016/j.jlp.2020.104095.

[34] A. Misuri, F. Ricci, R. Sorichetti, V. Cozzani, The effect of safety barrier degradation on the severity of primary NaTech scenarios, Reliab. Eng. Syst. Saf. 235 (2023) 109272, https://doi.org/10.1016/j.ress.2023.109272.

[35] L. Zhou, G. Chen, M. Zheng, X. Gao, C. Luo, X. Rao, Agent-based modelling methodology and temporal simulation for NaTech events in chemical clusters, Reliab. Eng. Syst. Saf. 243 (2023) 109888, https://doi.org/10.1016/j.ress.2023.109888.

[36] F. Ricci, M. Yang, G. Reniers, V. Cozzani, Emergency response in cascading scenarios triggered by natural events, Reliab. Eng. Syst. Saf. 243 (2024) 109820, https://doi.org/10.1016/j.ress.2023.109820.

[37] ISPRA, 2023. Inventario Seveso D.Lgs. 105/2015 [WWW Document]. Inventario degli stabilimenti a rischio di incidenti rilevanti connessi con sostanze pericolose. (Inventory of establishments with major-accident hazards involving hazardous substances). Istituto Superiore per La Protezione e la Ricerca Ambientale (ISPRA). URL https://www.rischioindustriale.isprambiente.gov.it/seveso-query-105/Default.php (accessed 6.19.23).

[38] A. Laurent, A. Pey, P. Gurtel, B. Fabiano, A critical perspective on the implementation of the EU Council Seveso Directives in France, Germany, Italy, and

Spain, Process Saf. Environ. Prot. 148 (2021) 47–74, https://doi.org/10.1016/j.psep.2020.09.064.
[39] V. Gallina, S. Torresan, A. Critto, A. Sperotto, T. Glade, A. Marcomini, A review of multi-risk methodologies for natural hazards: consequences and challenges for a climate change impact assessment, J. Environ. Manage. 168 (2016) 123–132, https://doi.org/10.1016/j.jenvman.2015.11.011.
[40] E. Pilone, P. Mussini, M. Demichela, G. Camuncoli, Municipal emergency plans in Italy: requirements and drawbacks, Saf. Sci. 85 (2016) 163–170, https://doi.org/10.1016/j.ssci.2015.12.029.
[41] D.J. Castro Rodriguez, J. Mietkiewicz, M. Vitale, G. Baldissone, M. Demichela, A. A. Barresi, NaTech triggered by lightning: novel insights from past events in the process industry, Heliyon 10 (11) (2024) e31610, https://doi.org/10.1016/j.heliyon.2024.e31610.
[42] D.J. Castro Rodriguez, J. Mietkiewicz, M. Vitale, G. Baldissone, M. Demichela, A. A. Barresi, Modelling industrial vulnerabilities to NaTech: methodological contributions from historical lightning triggered analysis., 2024, in: Collection of extended abstracts: Part 1 Advances in Reliability, Safety and Security. 34th European Safety and Reliability Conference (ESREL 2024). Polish Safety and Reliability Association, Jagiellonian University, 2024, pp. 17–18, 24–27 June, Cracow, Poland. Available on, https://esrel2024.com/wp-content/uploads/articles/ea1/modelling-industrial-vulnerabilities-to-natech-methodological-contributions-from-historical-lightning-triggered-analysis.pdf.
[43] E. Krausmann, E. Renni, M. Campedel, V. Cozzani, Industrial accidents triggered by earthquakes, floods and lightning: lessons learned from a database analysis, Nat. Hazards 59 (2011) 285–300, https://doi.org/10.1007/s11069-011-9754-3.
[44] E. Krausmann, K.-E. Köppke, R. Fendler, A.M. Cruz, S. Girgin, Chapter 8 - qualitative and semiquantitative methods for NaTech risk assessment, in: E. Krausmann, A.M. Cruz, E. Salzano (Eds.), NaTech Risk Assessment and Management, Elsevier, 2017, pp. 119–142, https://doi.org/10.1016/B978-0-12-803807-9.00008-5.
[45] V. Casson Moreno, G. Reniers, E. Salzano, V. Cozzani, Analysis of physical and cyber security-related events in the chemical and process industry, Process Saf. Environ. Protect. 116 (2018) 621–631, https://doi.org/10.1016/j.psep.2018.03.026.
[46] F. Ricci, V. Casson Moreno, V. Cozzani, A comprehensive analysis of the occurrence of NaTech events in the process industry, Process Saf. Environ. Prot. 147 (2021) 703–713, https://doi.org/10.1016/j.psep.2020.12.031.
[47] Istituto Nazionale di Statistica, 2013. La superficie dei comuni delle province e delle regioni italiane: dati al 9 ottobre 2011. (The area of municipalities in Italian provinces and regions: Data as of October 9, 2011) Statistiche Report. Istituto Nazionale di Statistica (Istat) Available on: https://www.istat.it/wp-content/uploads/2013/02/Superfici-dei-comuni.pdf.
[48] Carpanese, P., Badin, L., Follador, V., Ceresara, E.S., Donà, M., da Porto, F., 2024. Identification and Localization of Critical Industrial Assets in Italy, Book of abstracts. RETURN Dissemination workshop 1-2 February 2024. Torino, Italy. https://doi.org/10.5281/zenodo.10598007.
[49] Dipartimento della Protezione Civile, 2023. Classificazione sismica al 31 di marzo di 2023. (Seismic classification on March 31, 2023). Presidenza del Consiglio dei Ministri. Ufficio II-Attività Tecnico Scientifiche per la prevenzione dei Rischi-Servizio Rischio Sismico. URL: https://rischi.protezionecivile.gov.it/static/6cc491c88b2b6f59035ecba26d5afb1d/mappa-classificazione-sismica-agg-al-31-marzo-2023-formato-jpg.jpg.
[50] I. Vanzi, G.C. Marano, G. Monti, C. Nuti, A synthetic formulation for the Italian seismic hazard and code implications for the seismic risk, Soil Dyn. Earthq. Eng. 77 (2015) 111–122, https://doi.org/10.1016/j.soildyn.2015.05.001.
[51] P. Claps, G. Evangelista, D. Ganora, P. Mazzoglio, I. Monforte, FOCA: a new quality-controlled database of floods and catchment descriptors in Italy, Earth. Syst. Sci. Data 16 (2024) 1503–1522, https://doi.org/10.5194/essd-16-1503-2024.
[52] European Environment Agency, 2017. Number of landslides reported in Italy (1998-2001) — European Environment Agency. The European topic centre on land use and spatial information. URL: https://www.eea.europa.eu/data-and-maps/figures/number-of-landslides-reported-in-italy-1998-2001.
[53] European Environment Agency, 2024. Landslides in Italy. European Environment Agency. Graphic taken from Günther, A.; Reichenbach, P.; Hervás, J., 2008. Approaches for delineating areas susceptible to landslides in the framework of the European Soil Thematic Strategy. Proceedings of the First World Landslide Forum, Tokyo, 18-21 November 2008, pp. 235–238.URL: https://www.eea.europa.eu/data-and-maps/figures/number-of-landslides-reported-in-italy-1998-2001.
[54] M. Loche, M. Alvioli, I. Marchesini, H. Bakka, L. Lombardo, Landslide susceptibility maps of Italy: lesson learnt from dealing with multiple landslide types and the uneven spatial distribution of the national inventory, Earth. Sci. Rev. 232 (2022) 104125, https://doi.org/10.1016/j.earscirev.2022.104125.
[55] P. Salvati, C. Bianchi, M. Rossi, F. Guzzetti, Societal landslide and flood risk in Italy, Nat. Hazards Earth Syst. Sci. 10 (2010) 465–483, https://doi.org/10.5194/nhess-10-465-2010.
[56] Comitato Elettrotecnico Italiano, 2022. CEI PRODIS: "L'applicazione online del CEI che consente l'accesso ai dati di Densità Ceraunica." (CEI online application that provides access to Density Ceraunica data.) Comitato Elettrotecnico Italiano (CEI) URL: https://prodis.ceinorme.it/home.html?sso=y.
[57] R. Sabatino, A. Cordisco. Protezione contro i fulmini: valutazione del rischio., Dipartimento installazioni di produzione e insediamenti antropici. (Ligthning protection: risk assessment. Department of production installations and anthropogenic settlements), Istituto nazionale assicurazione contro gli Infortuni sul Lavoro INAIL, Milano, Italy, 2013.
[58] D.J. Castro Rodriguez, C. Tufano, M. Vitale, J. Mietkiewicz, G. Baldissone, A. Barresi, M. Demichela, Dataset: Natech events triggered by lightning within the process industry, Mendeley Data V1, (2023), https://doi.org/10.17632/fff64w3rzn.1. https://data.mendeley.com/drafts/fff64w3rzn.
[59] F. Ferlaino, A. Crescimanno, C.A. Dondona, L. Lella, F.S. Rota, Documento di Inquadramento Socioeconomico e Territoriale per il Piano Strategico della Città Metropolitana di Torino, Gruppo di ricerca IRES-Piemonte, Torino, Italia, 2015.
[60] S. Beltramino, M. Scalas, D.J. Castro Rodriguez, G. Brunetta, F. Pellerey, M. Demichela, A. Voghera, A. Longhi, G. Mutani, O. Caldarice, G. Miraglia, E. Lenticchia, L.L. Riccia, Assessing territorial vulnerability, TeMA - J. Land Use, Mobil. Environ. 15 (2022) 355–375, https://doi.org/10.6093/1970-9870/9069.
[61] D.J. Castro Rodriguez, A. Barresi, D. Demichela, A territorial view of the infrastructure resilience, in: Resilience Assessment: Methodological Challenges and Applications to Critical Infrastructures, Proceedings of the 63rd ESReDA Seminar, 2024, pp. 133–139, https://doi.org/10.2760/2808748. Joint Research Centre, Ispra, Italy, 25-26 October 2023. Kopustinskas, V., Foretic, H. and Asensio Bermejo, I. (Eds). Publications Office of the European Union, LuxembourgURL, https://data.europa.eu/doi/10.2760/2808748.
[62] D.J. Castro Rodriguez, M. Vitale, G. Baldissone, M. Demichela, A.A. Barresi, Insights into the vulnerability of the process industry against lightning strikes applied to the Italian context, Chem. Eng. Trans. 111 (2024) 595–600, https://doi.org/10.3303/CET24111100.
[63] Ricchiuti, A., Lotti, A., Astorri, F., Graziani, L., Maschio, G., Presti, G.L., Santucci, A., Ceci, P., Floridi, E., Favaroni, M., 2007. Mappatura del rischio industriale in Italia (No. APAT, Rapporti XX/2007). (Mapping Industrial Risk in Italy –No. APAT, Reports XX/2007–). Agenzia Nazionale per la Protezione dell'Ambiente e dei Servizi Tecnici (APAT).
[64] D.J. Castro Rodriguez, S. Beltramino, M. Scalas, E. Pilone, M. Demichela, Territorial representation of a vulnerability associated with the Seveso installations in a Nord Italian case study, in: Proceeding of the 32nd European Safety and Reliability Conference, Research Publishing Services, Dublin, Ireland, 2022, pp. 1463–1470, https://doi.org/10.3850/978-981-18-5183-4_R25-02-574-cd, 28th August –1st September.
[65] D.J. Castro Rodriguez, M. Demichela, S. Beltramino, M. Scalas, G. Brunetta, A. A. Barresi, Vulnerability scenario characterization in an industrial context using a NaTech indicator and a territorial multi-risk approach, in: Proceeding of the 33rd European Safety and Reliability Conference, 2023, pp. 2181–2188, https://doi.org/10.3850/978-981-18-8071-1_P187-cd, 3-7, September 2023.
[66] V. Cozzani, M. Campedel, E. Renni, E. Krausmann, Industrial accidents triggered by flood events: analysis of past accidents, J. Hazard. Mater. 175 (2010) 501–509, https://doi.org/10.1016/j.jhazmat.2009.10.033.
[67] A. Necci, E. Krausmann, NaTech Risk management– Guidance for Operators of Hazardous Industrial Sites and For National Authorities (JRC129450 No. EUR 31122 EN), Publications Office of the European Union, Luxembourg, 2022, https://doi.org/10.2760/666413.